Downloaded from https://www.lyellcollection.org by Imperial College of Science, Technology and Medicine on Jul 03, 2026

JGS
Journal of the Geological Society

Research article

https://doi.org/10.1144/jgs2025-214 | Vol. 183 | 2026 | jgs2025-214

A new source-to-sink synthesis of the Middle Triassic Helsby Sandstone Formation (Sherwood Sandstone Group) river system of the British Isles

Xiang Yan*, Gary J. Hampson and Alexander C. Whittaker

Department of Earth Science and Engineering, Imperial College London, London SW7 2AZ, UK
XY, 0009-0001-5167-3008; GJH, 0000-0003-2047-8469; ACW, 0000-0002-8781-7771
*Correspondence: Xiang.yan19@imperial.ac.uk

Abstract: Sediment grain size and mineralogy change in sediment routing systems from source to sink. A better understanding of sediment routing allows improved predictions to be made of the bulk grain size and mineralogy of sandstone fairways. We present a new appraisal of sediment routing in the Triassic Helsby Sandstone Formation (Sherwood Sandstone Group) and lowermost Mercia Mudstone Group of the British Isles, which constitute a key play for geological sequestration of CO_2. These strata were deposited and supplied by a major, north-flowing river system, which is traced from its source region in northern France to beyond the Irish Sea. We construct a new, integrated litho- and chronostratigraphic model to correlate key units across the British Isles. We then present sediment isopachs and volumes for this chronostratigraphic interval, and resolve palaeogeographical discrepancies using published sedimentological datasets, supplemented by a new synthesis of bulk sandstone mineralogy. Finally, we present a unified, updated sediment routing map for the Helsby Sandstone Formation. Substantial north–south differences in bulk sandstone mineralogy indicate that that sediment input from tributaries modified the composition of the Helsby Sandstone Formation along the course of the sediment routing system.

Supplementary material: A full dataset and further details are available at https://doi.org/10.6084/m9.figshare.c.8393428

Received 28 October 2025; **revised** 1 February 2026; **accepted** 15 March 2026

Sediment transport via rivers is a key surface process that transfers mass from sediment sources to sediment sinks. Source-to-sink systems can be divided into segments: areas of uplift and erosion where sediment is generated, areas of sediment bypass and transient storage, and subsiding depocentres (e.g. Sømme *et al*. 2009; Romans and Graham 2013; Helland-Hansen *et al*. 2016). The size, shape and distribution of sediment routing systems are controlled by their geomorphology (e.g. Sømme *et al*. 2009; Helland-Hansen *et al*. 2016; Markwick 2019), which is seldom completely preserved over deep time (Romans and Graham 2013; Helland-Hansen *et al*. 2016). Consequently, reconstructing palaeogeography is essential for constraining source-to-sink sediment routing in the geological record (e.g. Markwick 2019; Wrobel-Daveau *et al*. 2022). Understanding source-to-sink sediment routing is in turn a crucial tool to evaluate landscape responses to climate change and tectonics, as well as for predictive resource exploration (Wrobel-Daveau *et al*. 2022; Castelltort *et al*. 2023).

Source-to-sink sediment routing is commonly constrained by several methods, and involves the integration of lithostratigraphy, chronostratigraphy and palaeogeography, the last of these being constrained by methods including quantitative provenance analysis, sedimentology and palaeocurrent data (e.g. Morton and Hallsworth 1994; Hampson *et al*. 2014; Helland-Hansen *et al*. 2016; Michael and Zühlke 2022; Castelltort *et al*. 2023). Synthesizing these data can produce a defined stratigraphy and age model, sediment volumes and a defined map of sediment source areas and sinks.

The Triassic Sherwood Sandstone Group (SSG; Table 1) of the British Isles represents a regionally important, predominantly fluvial sediment routing system, dated to *c*. 249–240 Ma (Fig. 1a; Hounslow and McIntosh 2003; Hounslow and Gallois 2023). The SSG was deposited at low latitudes of *c*. 20°N during the early break-up of Pangaea (Fig. 1b) and in the aftermath of the Permo-Triassic extinction (Radley and Coram 2016; Newell 2017*a*, *b*). Much of the SSG is interpreted to have been laid down by major, north-flowing river systems that originated from Variscan highlands, now situated in northern France (Fig. 1c; e.g. Wills 1956; Burley 1987; Tyrrell *et al*. 2012; Morton *et al*. 2016; Newell 2017*a*; Burgess *et al*. 2025). The SSG has served as a key target for hydrocarbon exploration and production (e.g. Cowan 1993; McKie *et al*. 1997; Floodpage *et al*. 2001; Medici *et al*. 2019*a*; Scorgie *et al*. 2021) and for geothermal energy production (Downing *et al*. 1984; Knox *et al*. 1984), and is a major groundwater aquifer (Plant *et al*. 1999; Newell and Smith 2009; Medici *et al*. 2019*b*). More recently, the SSG has also become a key target for geological sequestration of CO_2 (e.g. Holliday *et al*. 1991; Newell and Shariatipour 2016; Scorgie *et al*. 2021; Chedburn *et al*. 2022; English *et al*. 2024; Gibson-Poole *et al*. 2026; Head *et al*. 2026). During the mid-Triassic, the SSG underwent a transition into the Mercia Mudstone Group (MMG), which forms the seal for the SSG reservoir (Fig. 1a; e.g. McKie *et al*. 1997; Scorgie *et al*. 2021; Chedburn *et al*. 2022; Hounslow and Gallois 2023; English *et al*. 2024).

The most recent holistic palaeogeography for this time interval, published more than 30 years ago, describes a major northward-directed sediment routing system originating from the remnant Variscan highlands of northern France, flowing through a series of linked extensional basins in the British Isles, into the East Irish Sea Basin (EISB) (Fig. 1c; Warrington and Ivimey-Cook 1992). This follows the older palaeogeographical interpretations of Wills (1970), Audley-Charles (1970) and Burley (1987). However, unlike previous interpretations, there is no mention or depiction of lateral sediment inputs, and sediment routing in the Wessex Basin and beyond the EISB remains unclear. Furthermore, the SSG–MMG transition is poorly understood. Finally, the

© 2026 The Author(s). This is an Open Access article distributed under the terms of the Creative Commons Attribution License (http://creativecommons.org/licenses/by/4.0/). Published by The Geological Society of London. Publishing disclaimer: https://www.lyellcollection.org/publishing-hub/publishing-ethics

Downloaded from https://www.lyellcollection.org by Imperial College of Science, Technology and Medicine on Jul 03, 2026

Table 1. List of commonly abbreviated stratigraphic and palaeogeographical terms used in text

Abbreviation	Full name
CHF	Chester Formation (Sherwood Sandstone Group)
EISB	East Irish Sea Basin
HSF	Helsby Sandstone Formation (Sherwood Sandstone Group)
MMG	Mercia Mudstone Group
MTU	Mid-Triassic Unconformity (former Hardegsen Unconformity)
SMF	Sidmouth Mudstone Formation (Mercia Mudstone Group)
SSG	Sherwood Sandstone Group
TSF	Tarporley Siltstone Formation (Mercia Mudstone Group)
WSF	Wilmslow Sandstone Formation (Sherwood Sandstone Group)

palaeogeographical extent of the catchments that sourced the fluvial systems of the SSG remains poorly constrained, as is their relation to the wider palaeogeography of NW Europe.

Integration of data and research that has become available since the publication of the work by Warrington and Ivimey-Cook (1992) could help to address these knowledge gaps. For instance, subsequent regional studies on the British Triassic system have collected and synthesized existing information to build basin-scale depositional models (e.g. Hamblin *et al.* 1992; Jackson *et al.* 1995; Plant *et al.* 1999; Dunford *et al.* 2001; Newell 2017*b*, 2023; Marsh *et al.* 2022), and quantitative provenance analysis has provided higher resolution constraints on sediment source areas and sediment routing within the SSG (Tyrrell *et al.* 2012; Morton *et al.* 2013, 2016). At the same time, better characterization of the pre-Triassic basement allows inferences to be made about source area composition (e.g. Baptiste 2016; Butler 2019). Emerging chronostratigraphy has allowed the improved correlation of coeval units both across the British Isles (Mange *et al.* 1999, 2007; Hounslow and McIntosh 2003; Hounslow *et al.* 2017; Hounslow and Gallois 2023) and to the wider European Triassic system (Bourquin *et al.* 2011; McKie 2017). Lastly, an improved understanding of the early Triassic climate (Péron *et al.* 2005; Ravidà *et al.* 2021) and tectonics (Newell 2017*a*) has offered further insights into controls on sediment generation.

Consequently, the last 30 years of research has resulted in a situation in which the SSG and MMG of the British Isles is locally well characterized in many aspects, yet is poorly resolved on the scale of the sediment routing system. The aim of this paper is to produce a comprehensive, up-to-date and quantitative reconstruction of this source-to-sink system, harmonized with the palaeogeography of NW Europe. To this end, we develop a unified lithostratigraphic and chronostratigraphic synthesis of key units in the SSG and MMG, focusing on a well-defined chronostratigraphic interval consisting of the upper SSG and lower MMG, in which the sediment routing system is well constrained. We present new maps of the sediment fairway using standardized nomenclature compiled from previous palaeogeographical studies. Using these products as a framework, we present the first quantitative estimates of the volume and distribution of fluvial and aeolian deposits within the fairway. We then derive isopach maps and volumes for units of interest, and we synthesize downsystem trends in sediment composition and provenance to characterize source-to-sink sediment routing, as well as the composition and extent of source areas. Finally, we use these data to evaluate the size and position of sediment inputs into the sediment routing system.

Geological framework

The British Triassic system begins during the lower Triassic with the SSG (Hounslow and McIntosh 2003), and passes into the MMG during the mid-Triassic (Fig. 1a; Hounslow and Gallois 2023). Deposition occurred in a series of linked, north–south-trending extensional basins throughout the British Isles, spanning the area between the English Channel and the Irish Sea (Warrington and Ivimey-Cook 1992). Deposition occurred under an arid and semiarid climate, as is widely indicated by sedimentology and palaeontology (e.g. Brookfield 2008; Evans *et al.* 2011; McKie 2014; Newell 2017*a*, *b*; Coram *et al.* 2019).

The standardized lithostratigraphy of the SSG, defined by the British Geological Survey (BGS; Ambrose *et al.* 2014), divides the group into three formations based on a succession typified in the Cheshire Basin. These three standardized formations are the conglomeratic and sandy fluvial Chester Formation (CHF), the mixed fluvial–aeolian Wilmslow Sandstone Formation (WSF) and

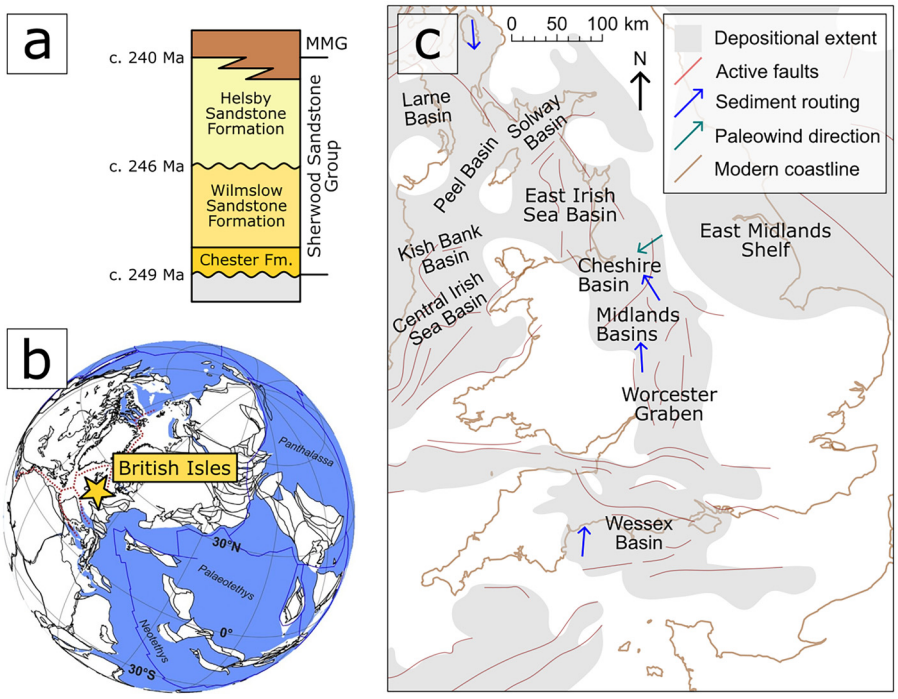


Fig. 1. (**a**) General stratigraphy and ages of the lower and middle Triassic succession of the British Isles, comprising the Sherwood Sandstone Group and Mercia Mudstone Group (MMG). (**b**) Global position of the British Isles during the early Triassic. (**c**) General basin configuration of the British Isles during the mid-Triassic. Source: (a) stratigraphy from Ambrose *et al.* (2014), ages from Hounslow and McIntosh (2003) and Hounslow and Gallois (2023); (b) adapted from Newell (2017*a*); (c) adapted from Warrington and Ivimey-Cook (1992).

Downloaded from https://www.lyellcollection.org by Imperial College of Science, Technology and Medicine on Jul 03, 2026

the fluvial–aeolian Helsby Sandstone Formation (HSF) (Fig. 2; Ambrose *et al*. 2014; Newell 2017*a*). Deposition of the HSF in the Wessex Basin and Worcester Graben was partially contemporaneous with the deposition of the lowermost MMG in the Cheshire Basin and EISB (Fig. 1a and c). The stratigraphy of the MMG is similarly standardized (Howard *et al*. 2008), and is represented by the Tarporley Siltstone Formation (TSF) and the Sidmouth Mudstone Formation (SMF) (Fig. 2; e.g. Warrington 1970*b*; Wilson 1990, 1993; Newell 2017*a*).

The BGS standardized stratigraphy supersedes older stratigraphic terminology, which differed between sedimentary basins. Unit names for basin-scale stratigraphy are presented in Figure 2 and are based on the synthesis of Howard *et al*. (2008) and Ambrose *et al*. (2014). Although the older, basin-scale terminology is still widely used (e.g. Newell 2017*a*, *b*; Scorgie *et al*. 2021; Chedburn *et al*. 2022; Marsh *et al*. 2022), the standardized BGS stratigraphy allows the SSG and MMG to be represented effectively on the source-to-sink scale, as it allows units to be robustly correlated between basins whilst avoiding any complex or redundant terminology.

The CHF (Fig. 1a) was deposited during the early Triassic by a regionally significant fluvial system sourced from the remnant Variscan mountains in northern France (e.g. Tyrrell *et al*. 2012; Morton *et al*. 2013, 2016). This system flowed northwards into the East Irish Sea Basin, possibly reaching Northern Ireland (Franklin *et al*. 2020; Moscardini *et al*. 2025). Deposition during the CHF occurred in a highly dynamic, but consistently hyperthermal semi-arid climate during the aftermath of the Permo-Triassic extinction (Sun *et al*. 2012), resulting in its unusually coarse grain size (Radley and Coram 2016; Newell 2017*a*).

The overlying WSF is conformable over the CHF (Figs 1a and 2), and is interpreted to represent a period of dominantly aeolian activity caused by accelerated extensional faulting, resulting in the disconnection of basins and dissection of the SSG fairway (Newell 2017*a*). The boundary between the WSF and the overlying HSF is largely unconformable (Fig. 2), representing a period of tectonic uplift traditionally attributed to the Europe-wide Hardegsen tectonic event (Evans *et al*. 1993; Mange *et al*. 1999, 2007; Bourquin *et al*. 2011).

The HSF (Fig. 1a) represents a second, mid-Triassic interval of fluvial activity (Newell 2017*a*, *b*). The HSF was deposited in a more stable, albeit still semiarid climate (Newell 2017*a*) coinciding with a biotic recovery (Benton and Spencer 1995; Coram *et al*. 2019). The mid-Triassic then saw a gradual, diachronous aridification, with the river systems of the HSF retreating southwards. Fluvial–aeolian deposition was replaced by the playa lakes and marine evaporites of the MMG, initially in the EISB (Fig. 1a; e.g. Greenwood and Habesch 1997; Jackson *et al*. 1995; Plant *et al*. 1999; McKie 2017) until fluvial activity finally ceased in the Wessex Basin (Newell 2017*b*; Hounslow and Gallois 2023).

Deposition of the CHF and HSF has previously been attributed to the 'Budleighensis' River (*sensu* Wills 1956, 1970, 1976). This was interpreted to be a regionally significant river system sourced from the Variscan massifs of northern France (Tyrrell *et al*. 2012; Morton *et al*. 2013, 2016), which flowed into the EISB towards Ireland (e.g. Dunford *et al*. 2001; Franklin *et al*. 2020; Moscardini *et al*. 2025). The drainage scale of this fluvial system, approximately 1000 km, would be comparable with the modern Ebro River in Spain (Helland-Hansen *et al*. 2016). Substantial changes in sediment mineralogy occur between the Wessex Basin and the East Irish Sea Basin (Fig. 1c; Burley 1987; Plant *et al*. 1999; Morton *et al*. 2013), and it remains unclear how important the northern France source area was for the sediment routing system, relative to other potential sediment inputs. In the CHF, it has been proposed that variations in clast concentration suggest substantial sediment inputs occurring downstream of the northern France source area (Burgess *et al*. 2025).

In the context of NW Europe, the northern France source area is known as the Gallic Massif (*sensu* Sass *et al*. 2023), a major upland region encompassing the modern-day Variscan–Cadomian-aged Armorican Massif, the French Massif Central and the buried basement surrounding them, under the Paris Basin and English Channel. The north-flowing 'Budleighensis' system shared a Gallic Massif source area with two other substantial fluvial systems: an east-flowing system that deposited the Buntsandstein in France and Germany (the 'Alemania' river, *sensu* Ravidà *et al*. 2021), and a SE-directed system that deposited the Buntsandstein in Iberia (e.g. Bourquin *et al*. 2011; Sánchez Martínez *et al*. 2012; McKie 2017).

The SSG exists in tectonostratigraphic continuity with underlying Permian aeolian sandstones and playa lake mudstones, which represent the first significant basin fill after the extensional collapse of the Variscan Orogeny (e.g. Hamblin *et al*. 1992; Jackson *et al*. 1995; Newell 2017*a*), as well as the overlying MMG (e.g. Howard *et al*. 2008; Hounslow *et al*. 2017; McKie 2017). The post-depositional history of the SSG is variable between basins; however, the unit has generally undergone 2–4 km of burial across the UK (e.g. Carter *et al*. 1995; Mikkelsen and Floodpage 1997; Bray *et al*. 1998; Pharaoh *et al*. 2019). The northern section of the SSG fairway, particularly in NW England and offshore in the Irish Sea, has additionally seen substantial exhumation and erosion during the Cenozoic, bringing the SSG to outcrop (e.g. Mikkelsen and Floodpage 1997; Pharaoh *et al*. 2019).

Overall, four uncertainties remain in characterizing the SSG of the British Isles, which this study addresses. First, the chronostratigraphy of the SSG and lower MMG is not rigorously integrated with the existing lithostratigraphy across the British Isles. Second, its sediment fairway and depositional volumetrics have not been mapped out or quantified. Third, variations in bulk sandstone mineralogy must be appraised down the sediment fairway. Finally, sediment routing and source areas must be reappraised using updated, published data. We seek to address these research needs in this study.

Methods

A synthesis of the lithostratigraphy of the HSF, TSF and lower SMF was completed to correlate units between sedimentary basins in the British Isles. Chronostratigraphy was synthesized using the magnetostratigraphically constrained section of the HSF in the Wessex Basin (Hounslow and McIntosh 2003; Hounslow and Gallois 2023) and an equivalent section in the EISB (Mange *et al*. 1999; Hounslow and McIntosh 2003), which were then correlated to the global Triassic timescale (Ogg *et al*. 2020). These sections are then supplemented by published palynology and the correlation of lithostratigraphic units and boundaries across the HSF, TSF and lower SMF. From this lithostratigraphic and chronostratigraphic model, a single, time-equivalent interval could then be defined across the British Isles as a basis for further spatial, volumetric and palaeogeographical analysis. This studied interval spans 5 Myr, from 246.5 to 241.5 Ma, as detailed below.

To map the fairway of this chronostratigraphically defined interval, a geological database was compiled from published outcrop sections and borehole logs, and borehole records held by the BGS Onshore Single Borehole Index, the Bureau de Recherches Géologiques et Minières, the UK Onshore Geophysical Library and the North Sea Transition Authority National Data Repository (n = 393). For data points where stratigraphic units were completely preserved and not truncated by erosion, unit thicknesses and dominant lithologies were recorded. Boreholes were also recorded where the defined stratigraphic interval was not deposited, delimiting the edge of the fairway (Fig. 3). In areas where data points were too dense to manually parse or where sources offered contradictory interpretations, published interpretations were given

Downloaded from https://www.lyellcollection.org by Imperial College of Science, Technology and Medicine on Jul 03, 2026

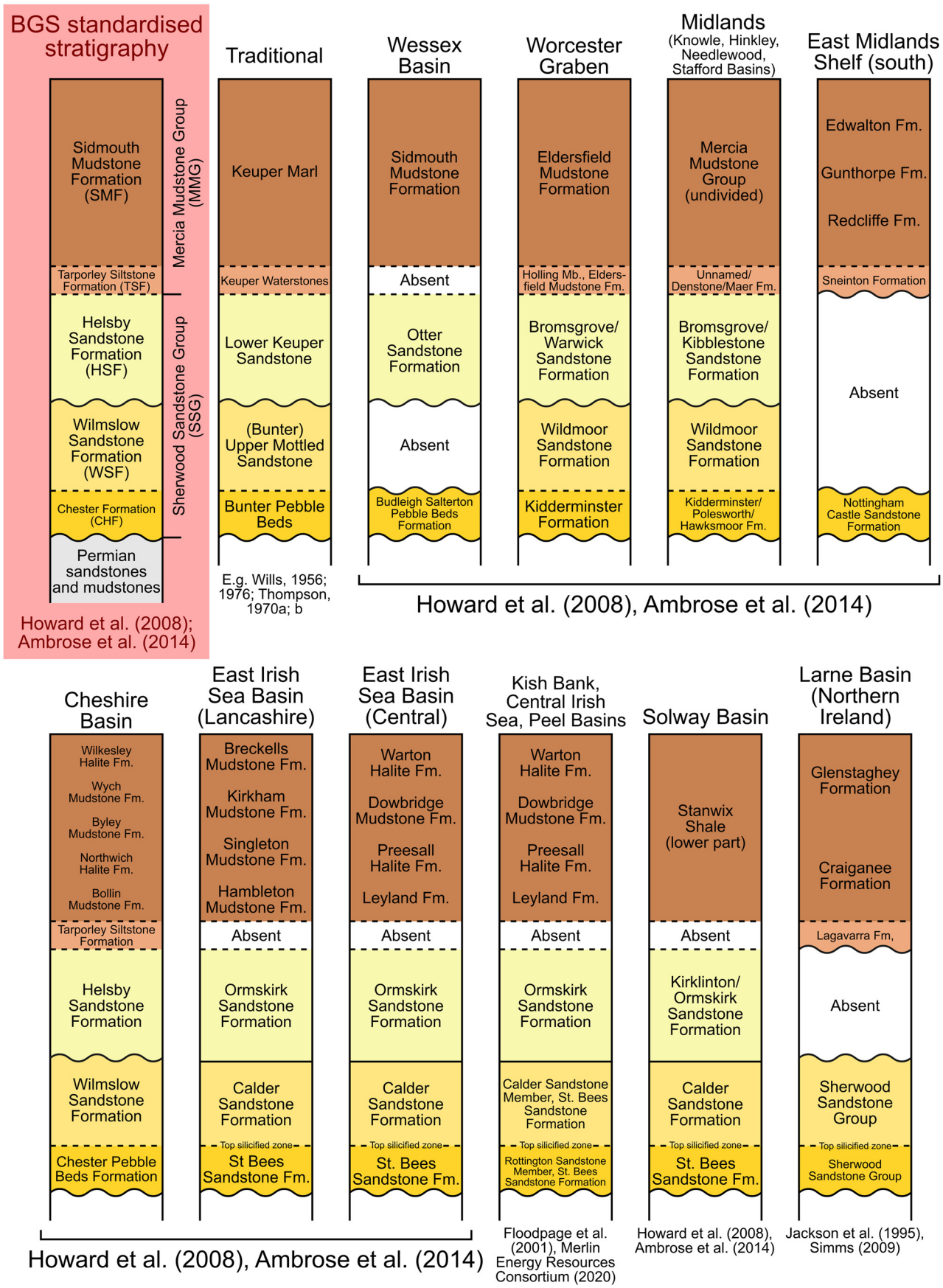


Fig. 2. Commonly used regional lithostratigraphic terms for the Sherwood Sandstone Group and Mercia Mudstone Group correlated to the BGS revised standardized stratigraphy in Britain. Source: a comprehensive review of SSG and MMG regional terminology has been provided by Ambrose *et al.* (2014) and Howard *et al.* (2008) , respectively.

Downloaded from https://www.lyellcollection.org by Imperial College of Science, Technology and Medicine on Jul 03, 2026

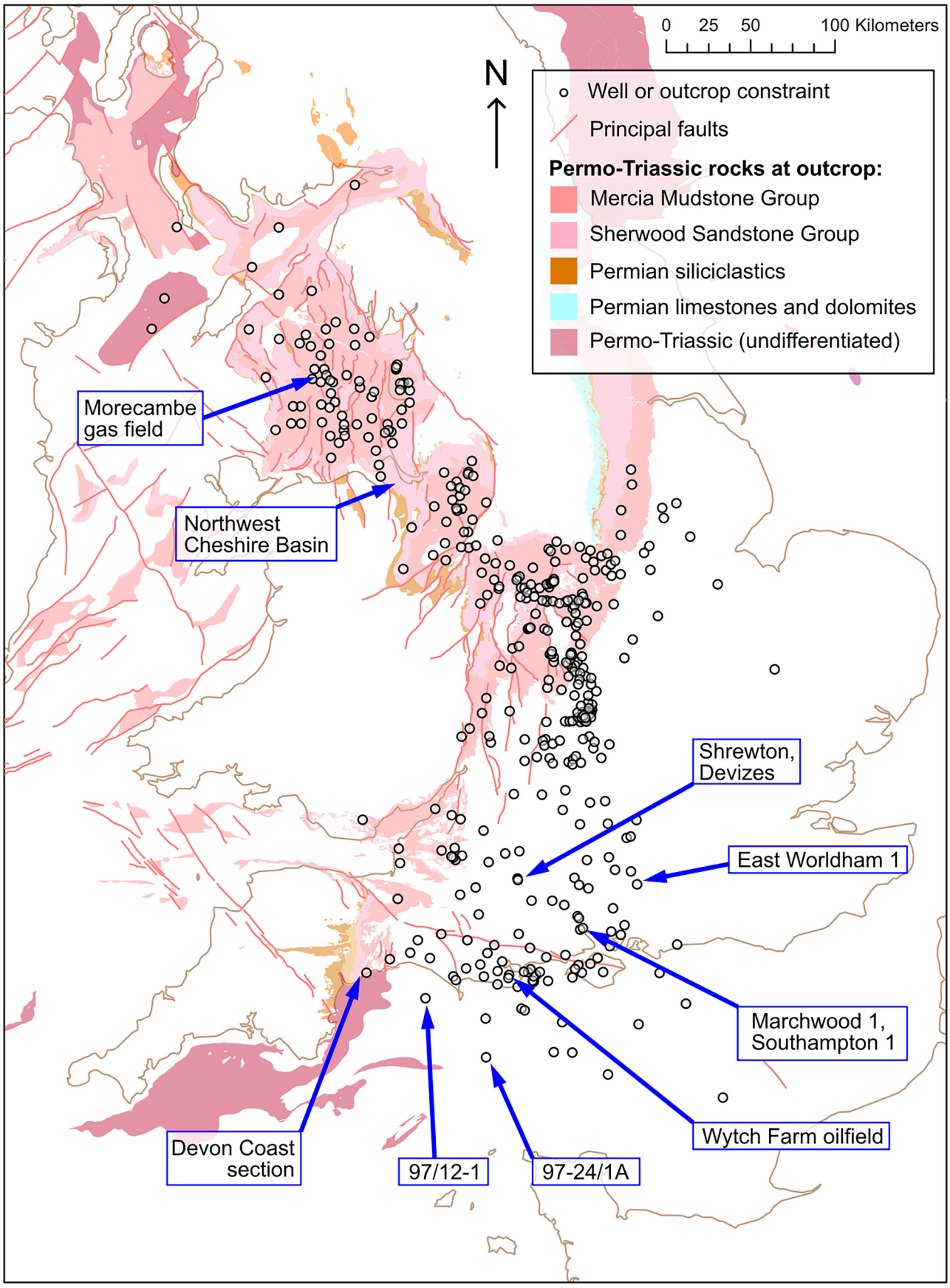


Fig. 3. Data framework composed of analysed boreholes and outcrops, overlaid on Permo-Triassic outcrop geology and structure of the British Isles. Labelled locations are mentioned in the text. Source: Geological Map Data BGS © UKRI 2025.

priority. In the absence of any existing interpretations, original interpretations were made using wireline logs and lithological data. The sediment fairway was then mapped from these data. Where data were sparse or absent, or where the SSG was absent owing to post-depositional erosion, the fairway was mapped based on existing geological constraints and palaeogeographical interpretations.

Downloaded from https://www.lyellcollection.org by Imperial College of Science, Technology and Medicine on Jul 03, 2026

Table 2. Key sedimentological parameters for the Helsby Sandstone Formation (HSF) in each sedimentary basin in the mapped fairway (Fig. 3)

Basin	Wessex	Worcester	Midlands	Cheshire	East Irish Sea
Median porosity (%)	18.0	14.8	26.9	24.0	12.7
Proportion of fluvial deposits (%)	90	100	100	71	64
Proportion of aeolian deposits (%)	10	0	0	29	36

Median porosities compiled by Medici *et al.* (2019*a*), except the Wessex Basin (estimated from Bowman *et al.* 1993; Newell and Shariatipour 2016). Estimated proportion of fluvial and aeolian deposits compiled from Thompson (1970*a*), Meadows and Beach (1993*b*), McKie *et al.* (1997), Ambrose *et al.* (2014) and Newell (2017*b*).

The resulting sediment fairway map was then integrated with nomenclature for sedimentary basins, palaeohighs and major structural features from existing palaeogeographical reconstructions (e.g. Wills 1956, 1970; Audley-Charles 1970; Burley 1987; Warrington and Ivimey-Cook 1992; Bourquin *et al.* 2011; Newell 2017*a*) to create a full palaeogeographical framework for the middle Triassic of the British Isles. Our reconstruction addresses major unknowns in fairway extent and reconciles inconsistencies between previous interpretations.

Where the sediment fairway was sufficiently constrained by thickness data (Fig. 3), stratigraphic thicknesses were combined with a series of points where deposition is inferred to be absent (n = 32), representing nondeposition around Triassic massifs from the previously developed palaeogeographical framework. These points were collectively interpolated with a regional fault map based on BGS data (DiGRock625k 2008; DiGRock250k 2013) and Newell (2017*b*) to produce isopach maps for each studied lithostratigraphic unit. From these isopach maps, resulting sedimentary rock volumes were then computed for each basin, and were converted to solid rock volumes by removing pore space, a parameter well constrained by previous studies. For the HSF, we used porosity estimates compiled by Medici *et al.* (2019*a*) for the EISB, Cheshire, Midlands and Worcester basins (Table 2). Porosity for the Wessex Basin is estimated at 18% (Table 2; Bowman *et al.* 1993; Newell and Shariatipour 2016). The same value of porosity is assigned to both aeolian and fluvial deposits in the HSF in each basin. For the MMG, mean values of 14.9% for the TSF and 17.8% for the SMF (Parkes *et al.* 2021) were applied for all basins. The Preesall and Northwich Halites are assumed to have zero porosity.

Fluvial and aeolian HSF volumes were estimated from literature-derived basin-scale sedimentological trends. Previous basin-scale estimates of the proportion of fluvial deposits were calculated by Medici *et al.* (2019*a*), but were limited to outcrop observations and are therefore biased to basin margins. Furthermore, as their method of calculation is not explicit, it is challenging to verify these estimates. We provide new estimates for the proportion of fluvial deposits based on basin-scale sedimentological trends derived from published outcrop, borehole and seismic data. Three depositional environments are recognized: fluvial, aeolian and fluvial–aeolian. For each basin, these depositional environments are used to calculate the proportion of two deposit types: fluvial and aeolian. Fluvial depositional environments are considered to have a fluvial deposit content of 100%. Aeolian depositional environments are considered to have an aeolian deposit content of 100%. Fluvio-aeolian environments, where fluvial and aeolian strata coexist in close succession, are inferred to contain 50% fluvial deposits and 50% aeolian deposits, the most probable representative value. These derived proportions are then used to calculate the overall basin-scale volume of fluvial and aeolian deposits.

Petrographic data for bulk sandstone mineralogy in the HSF were compiled from seven sources across 16 localities in the sediment fairway, resulting in 320 data points. These data cover both borehole and outcrop localities, and represent either fluvial or aeolian facies (Ali 1982; Knox *et al.* 1984; Burley 1987; Chisholm *et al.* 1988; Svendsen and Hartley 2001; Meadows 2004; Scorgie *et al.* 2021; De Sainz Simpson 2022; a full dataset is provided in Supplementary material 4). Owing to historical differences in point counting technique (e.g. Garzanti 2019; Augustsson 2021), these data cannot be compared as a single group but must be divided by method: Indiana and Gazzi–Dickinson, based on their classification of rock fragments (see supplementary material 4 for more detail). For each point counting method, data were grouped by basin, and then separated by aeolian and fluvial deposits to characterize the bulk mineralogical variability of sandstones within the sediment fairway. Sediment mineralogy within the HSF has also been studied in the context of quantitative provenance analysis (e.g. Plant *et al.* 1999; Tyrrell *et al.* 2012; Morton *et al.* 2013, 2016). These studies are equally important in constraining sediment routing and source areas, and are discussed separately in the basin-by-basin synthesis of sediment routing (see below).

Although the bulk mineralogy of the lower MMG has also been studied in its sand fraction (Scorgie *et al.* 2021; de Sainz-Simpson 2022) and silt–clay fraction (Jeans 2006; Armitage *et al.* 2013; Jones *et al.* 2025), interpreting sediment routing in the MMG is problematic. There are no sediment provenance studies to support compositional data, and understanding of depositional environments in the MMG in the Cheshire Basin and EISB remains limited. For the purposes of this study, we hence focus on sediment mineralogy in the HSF. A first-order synthesis of diagenesis was then compiled to assess its impact on detrital mineralogy. This was then generalized throughout the fairway by using a compilation of burial histories for each basin. From this, the detrital mineralogy of the HSF in each basin could be characterized, and fairway-scale trends in bulk sandstone mineralogy in the HSF could be assessed.

Basin-level sedimentological data were then synthesized to reconstruct fairway sediment routing. First, published basin-scale studies characterizing the HSF and lower MMG were collated. For each basin, previously documented palaeocurrents, sedimentological trends and quantitative provenance analysis results were catalogued. These datasets were further complemented by the new synthesis of bulk sandstone mineralogy, as well as the compilation of predominant lithologies from borehole logs (Fig. 3). For each basin, a map of dominant lithofacies could then be created by plotting sedimentological trends and borehole lithological data within the previously established fairway limits. Sediment routing directions were determined from representative palaeocurrent indicators, basin-scale sedimentological trends and quantitative provenance analysis. Sediment inputs into the system were inferred using quantitative provenance analysis and our synthesis of bulk sandstone mineralogy. Where present, the degree of fluvial–aeolian interaction was also inferred from the synthesis of bulk sandstone mineralogy. Basin-level sediment routing was then linked together to provide a harmonized record of sediment routing within the whole fairway.

Using the previously developed palaeogeographical and sediment routing framework, emergent uplands across NW Europe were then lithologically and, where possible, topographically characterized. Sediment routing for the HSF was then integrated with existing constraints on sediment routing in northeastern Iberia and NW Europe to produce a regionally consistent map of sediment sourcing. By constraining the extent and coverage of non-preserved drainage in the source areas of the HSF, the source-to-sink system could be fully characterized.

Downloaded from https://www.lyellcollection.org by Imperial College of Science, Technology and Medicine on Jul 03, 2026

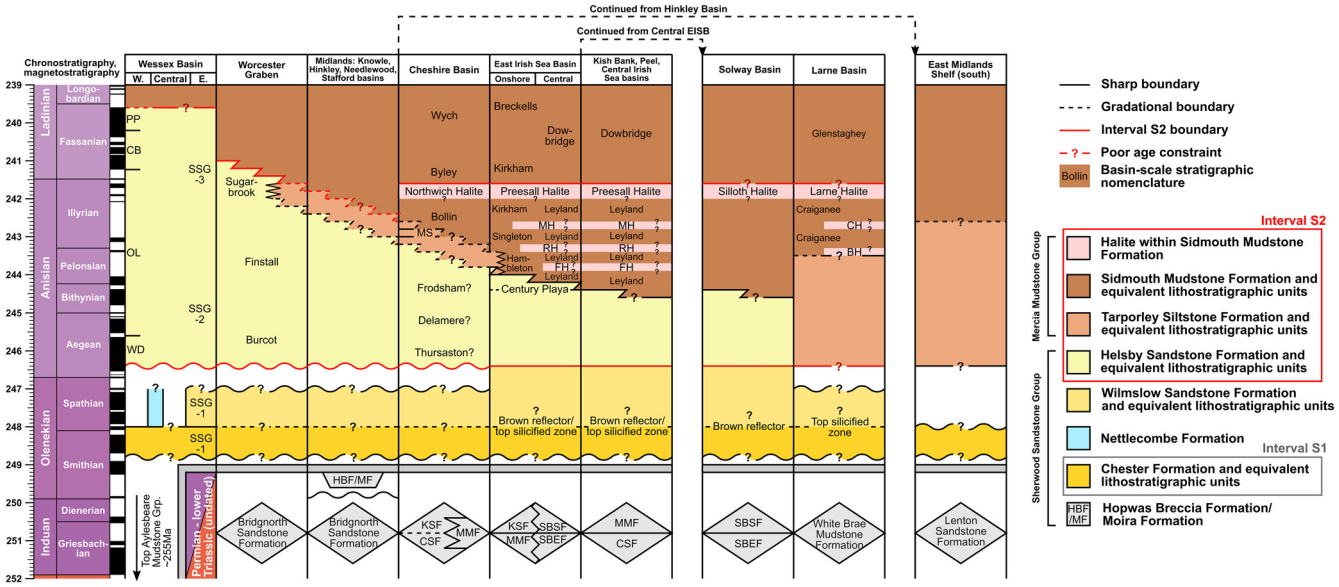


Fig. 4. Integrated lithostratigraphic and chronostratigraphic correlation for the Permian to middle Triassic System in the British Isles, including undated Permo-Triassic units, the Sherwood Sandstone Group and lower Mercia Mudstone Group. Basins are ordered from SE to NW. PP, Pennington Point Member; CB, Chiselbury Bay Member; OL, Otterton Ledge Member; WD, West Down Member; MS, Malpas Sandstone Member; MH, Mythrop Halite Member; RH, Rossall Halite Member; FH, Fylde Halite Member; CH, Carnduff Halite Member; BH, Ballybolley Halite Member; KSF, Kinnerton Sandstone Formation; MMF, Manchester Marls Formation; CSF, Collyhurst Sandstone Formation; SBSF, St Bees Shale Formation; SBEF, St Bees Evaporites Formation. Source: chronostratigraphic and magnetostratigraphic timescale adapted from Ogg *et al.* (2020).

Stratigraphy

Revised terminology

Table 1 lists commonly abbreviated stratigraphic and geographical terms. The 'Budleighensis River' (*sensu* Wills 1956) was conceived as the main, north-flowing river, which brought the distinctive quartzite clasts of the CHF from a southern Variscan source area into the Midlands. Since then, the term 'Budleighensis' has expanded to encompass all fluvial activity occurring within the CHF and HSF (e.g. Plant *et al.* 1999; Tyrrell *et al.* 2012; Radley and Coram 2016; Newell 2017*a*; Franklin *et al.* 2020; Burgess *et al.* 2025). This is problematic, as the CHF and the HSF represent temporally and sedimentologically distinct river systems (e.g. Hounslow and McIntosh 2003; Morton *et al.* 2013; Newell 2017*a*). Further, multiple tributaries and bifurcations have been interpreted for these river systems (e.g. Smith and Edwards 1991; Morton *et al.* 2016; Burgess *et al.* 2025; Gibson-Poole *et al.* 2026). Nomenclature that is more spatially generic but temporally rigorous is necessary to represent these source-to-sink systems. We henceforth refer to this system as a whole as the 'Sherwood River System', with the 'Sherwood-1 River System' referring to the rivers of the CHF and the 'Sherwood-2 River System' referring to the rivers of the HSF.

We adopt the term Mid-Triassic Unconformity (*sensu* Newell 2017*a*) for the early Anisian unconformity below the HSF (Fig. 4). Its former name, the Hardegsen Unconformity (e.g. Ambrose *et al.* 2014), is misleading, as although it was probably caused by the same regional tectonic event, the Franco-German Hardegsen Unconformity is distinctly older than its British equivalent (Hounslow and McIntosh 2003). The new terminology avoids any implied time equivalence between the two.

Lithostratigraphy

Our lithostratigraphic synthesis (Fig. 4) builds on the standardized nomenclature of Howard *et al.* (2008) and Ambrose *et al.* (2014). The stratigraphy in Figure 4 is arranged by depocentre from south to north; that is, down the depositional system. Basin-scale lithostratigraphic divisions are depicted to aid correlation, and to illustrate the spatio-temporal evolution of the SSG and MMG. Although the correlations of Howard *et al.* (2008) and Ambrose *et al.* (2014) terminate in the EISB and Solway Basin respectively, the SSG and lower MMG can be correlated further (e.g. Jackson *et al.* 1997; Mange *et al.* 1999, 2007; Simms 2009) and we integrate these areas into our stratigraphic framework.

On the largest scale, the SSG is divided into four formations in accordance with Ambrose *et al.* (2014): the Hopwas Breccia Formation, the CHF, WSF and HSF. The lower MMG, in accordance with Howard *et al.* (2008), is divided into the TSF and the SMF (Fig. 4). The SSG overlies various Permo-Triassic units that represent the initial, post-Variscan basin fill.

The HSF represents the second period of fluvial activity within the SSG. In the western Wessex Basin, the HSF is divided into four well-characterized members at outcrop (Fig. 4; Newell 2017*b*). The HSF lies over a prominent ventifact horizon developed at the top of the CHF, a manifestation of the Mid-Triassic Unconformity (Hounslow and McIntosh 2003). In the Central Wessex Basin, no formal lithostratigraphic divisions exist, although in the Wytch Farm oilfield the HSF has previously been split into five units separated by widespread floodplain–playa deposits (McKie *et al.* 1997). In the Southampton 1 borehole, the HSF is divided into two members by lithology (Thomas and Holliday 1982) and heavy mineral composition (Fig. 4; Morton *et al.* 2016).

In the Worcester Graben, the HSF is divided into three members by lithology (Fig. 4 ; Old *et al.* 1991; Barclay *et al.* 1997; Sumbler *et al.* 2000). The HSF here passes gradationally upwards and northwards into the TSF, which in turn grades into the SMF. The HSF remains undivided in the Knowle, Needlewood, Hinkley and Stafford Basins of the Midlands, and similarly grades into the TSF and then the SMF (Fig. 4).

The HSF is absent from the East Midlands Shelf. Instead, a ventifact horizon, marking the Mid-Triassic Unconformity, lies on top of the CHF (Burley 1987; Newell 2023). This is in turn overlain by the MMG, which has a well-defined stratigraphy in this area (Howard *et al.* 2008). It is suggested that tectonic activity associated with the Mid-Triassic Unconformity uplifted the Pennine–

Downloaded from https://www.lyellcollection.org by Imperial College of Science, Technology and Medicine on Jul 03, 2026

Charnwood Ridge, preventing the Sherwood-2 River System flowing NE (Warrington and Ivimey-Cook 1992; Ambrose *et al.* 2014; Newell 2017*a*, 2023). The East Midlands Shelf became reconnected to the Hinkley Basin during the late Anisian, towards the top of the studied interval (Ambrose *et al.* 2014; Jones *et al.* 2025).

In the Cheshire Basin, the HSF is typically divided into the fluvio-aeolian Thurstaston Member, the fluvial Delamere Member and the fluvio-aeolian Frodsham Member (Fig. 4; Ambrose *et al.* 2014). It is likely that these members represent large-scale, interdigitating facies associations (Thompson 1970*a*; Burley 1987; Plant *et al.* 1999). In the NW Cheshire Basin (Fig. 3), the lower boundary of the HSF may lie at the base of the Delamere Member, with the previously identified Thurstaston Member being part of the WSF instead (Earp and Taylor 1986; Hough 2002). The HSF grades into the TSF, which locally contains the aeolian Malpas Sandstone Member (Fig. 4; e.g. Wilson 1993; Jackson *et al.* 1995; Mikkelsen and Floodpage 1997; Plant *et al.* 1999). The TSF then grades into the SMF (Plant *et al.* 1999). The Northwich Halite Member lies within the SMF and forms a lithologically uniform marker unit across the basin (Fig. 4; e.g. Evans and Holloway 2009; Evans *et al.* 2011).

In the EISB, the Mid-Triassic Unconformity disappears (Jackson *et al.* 1995), and the HSF and WSF appear conformable (Fig. 4). No accepted division of the HSF exists on a basin scale. The HSF has been variously divided into two or three members (Jackson *et al.* 1997). In the Morecambe Gas Field (Fig. 3), the HSF is split into four members, following the tripartite stratigraphy of the HSF in the Cheshire Basin with the addition of the Waterstones Member (Bushell 1986). However, any stratigraphic equivalence implied by the assignment of members is misleading, because these members represent large-scale, interdigitating facies associations, as previously noted for the HSF in the Cheshire Basin (Meadows and Beach 1993*b*). The isochronous and widespread 'Century Playa' interval (Fig. 4; Thompson and Meadows 1997; Meadows 2006) is the only consistent, correlatable unit occurring within the HSF. The contact between the top of the HSF and the overlying MMG is sharp. The TSF is present only in the southeastern part of the EISB (Burley 1987; Scorgie *et al.* 2021), and the SMF directly overlies the HSF elsewhere (Fig. 4). The stratigraphic nomenclature of the MMG differs between the offshore basin centre and onshore eastern basin margin, but strata in these locations are directly correlatable. For example, the Preesall, Mythrop and Rossall Halites are directly equivalent in both regions (Figs 2 and 4). The Preesall Halite is also the lateral equivalent of the Northwich Halite of the Cheshire Basin (Fig. 4; Jackson *et al.* 1995; Howard *et al.* 2008).

In the Peel, Kish Bank and Central Irish Sea basins, the Ormskirk Sandstone Formation is equivalent to the HSF in the EISB (Fig. 4; Mange *et al.* 1999, 2007; Floodpage *et al.* 2001; Merlin Energy Resources Consortium 2020). The Leyland Formation and Preesall Halite of the MMG also correlate to their equivalents in the EISB (Chadwick *et al.* 2001; Merlin Energy Resources Consortium 2020). In the Solway Basin, the HSF is undivided (Fig. 4; Ambrose *et al.* 2014). The Silloth Halite is equivalent to the Preesall and Northwich Halites in the EISB and Cheshire Basin (Jackson *et al.* 1995; Floodpage *et al.* 2001; Fig. 4).

In the Larne Basin of Northern Ireland, HSF-equivalent units are absent, and instead the siltstone-rich Lagavarra Formation is present above the Mid-Triassic Unconformity (Fig. 4, e.g. Jackson *et al.* 1995; Simms 2009). The Larne Halite of the SMF is probably correlative with the Preesall and Northwich Halites of the EISB and Cheshire Basin, respectively (Jackson *et al.* 1995).

Chronostratigraphy

The base of the HSF (i.e. the Mid-Triassic Unconformity and its correlative conformities; Fig. 4) is magnetostratigraphically dated to the lower Anisian in both the Wessex Basin and the EISB (Hounslow and McIntosh 2003). This boundary is thus an approximately isochronous surface, dated at *c.* 246.5 Ma (Ogg *et al.* 2020).

The top of the HSF (i.e. the SSG–MMG boundary) is widely documented to become progressively older to the north (Fig. 4). At the Devon Coast section in the Wessex Basin, this boundary is magnetostratigraphically dated to the lower Ladinian (Hounslow and Gallois 2023), at *c.* 239.6 Ma (Ogg *et al.* 2020). In the Worcester Graben, palynology puts the upper part of the HSF within the Anisian or possibly the lower Ladinian, with the SMF being Ladinian in age. (Fig. 4; Barclay *et al.* 1997). In the Midlands, palynology suggests that the lower SMF is Anisian in age (Fig. 4; Bridge and Hough 2002). In the East Irish Sea Basin, magnetostratigraphy suggests that the top of the HSF is mid-Anisian in age (lower Pelonsian; Hounslow and McIntosh 2003), at *c.* 244 Ma (Ogg *et al.* 2020, Fig. 4). On the East Midlands Shelf, the HSF is absent, although palynology suggests that the TSF is Anisian in age (Howard *et al.* 2008).

Within the MMG of the Cheshire and East Irish Sea basins, the Northwich and Preesall Halites (Fig. 4) are interpreted to record marine transgressions (Greenwood and Habesch 1997; Thompson and Meadows 1997) and their top provides an isochronous surface of upper Anisian age (Jackson *et al.* 1995; Evans *et al.* 2011; Chedburn *et al.* 2022). The Anisian–Ladinian boundary (*c.* 241.5 Ma; Ogg *et al.* 2020) is constrained by palynology and lies just above this marker unit, within the upper Byley Mudstones in the Cheshire Basin and within the lower Kirkham Mudstones in the EISB (Fig. 4; Wilson and Evans 1990; Plant *et al.* 1999). The Silloth and Larne Halites in the Solway and Larne basins are thought to be correlative to the Preesall and Northwich Halites (Jackson *et al.* 1995), and therefore are of equivalent age (Fig. 4).

From these chronostratigraphic constraints, a single, roughly time-equivalent interval, Interval S2, defined in duration by activity of the Sherwood-2 River System, can be projected along the sediment routing system. The base of S2 (Fig. 4, *c.* 246.5 Ma; Ogg *et al.* 2020) is taken at the Mid-Triassic Unconformity between the Wessex Basin and Cheshire Basin, and its correlative conformity (the HSF–WSF boundary) in the East Irish Sea, Solway, Kish Bank, Peel and Central Irish Sea basins (Fig. 4). In Northern Ireland, the base of S2 is taken as the unconformity at the base of the TSF. The top of Interval S2 follows the Anisian–Ladinian boundary (*c.* 241.5 Ma; Ogg *et al.* 2020) as closely as possible, but is defined separately for each basin. In the Wessex Basin, the top S2 boundary follows the HSF–SMF boundary, which is lower Ladinian in age (Hounslow and Gallois 2023), *c.* 239.6 Ma (Ogg *et al.* 2020). The true Anisian–Ladinian boundary is within the upper Otterton Ledge Member of the HSF in the western Wessex Basin (Hounslow and Gallois 2023); however, the absence of correlation elsewhere in the Wessex Basin prevents this boundary from being used (Fig. 4). In the Worcester Graben, the Midlands and the East Midlands Shelf, we use the TSF–SMF boundary as the top S2 boundary. This boundary is roughly of Anisian–Ladinian age in the Worcester Graben. Although the boundary becomes older in the Midlands and the East Midlands Shelf, the absence of more distinctive stratigraphic markers within the SMF means that the top of the TSF remains the best option for correlation (Fig. 4). In the Cheshire Basin, EISB and further north, the top of S2 is taken at the top of the Northwich and Preesall Halite Members of the SMF and their stratigraphic equivalents, which are late Anisian in age (Fig. 4).

In summary, Interval S2 encompasses the HSF, the TSF and the SMF up to and including the Preesall and Northwich Halites and their stratigraphic equivalents. Interval S2 has a duration of approximately 5 Myr, but this may be longer in the Wessex Basin (*c.* 6.9 Ma), and shorter in the Midlands Basins (Fig. 4). This time-defined stratigraphic interval serves as an important framework for

Downloaded from https://www.lyellcollection.org by Imperial College of Science, Technology and Medicine on Jul 03, 2026

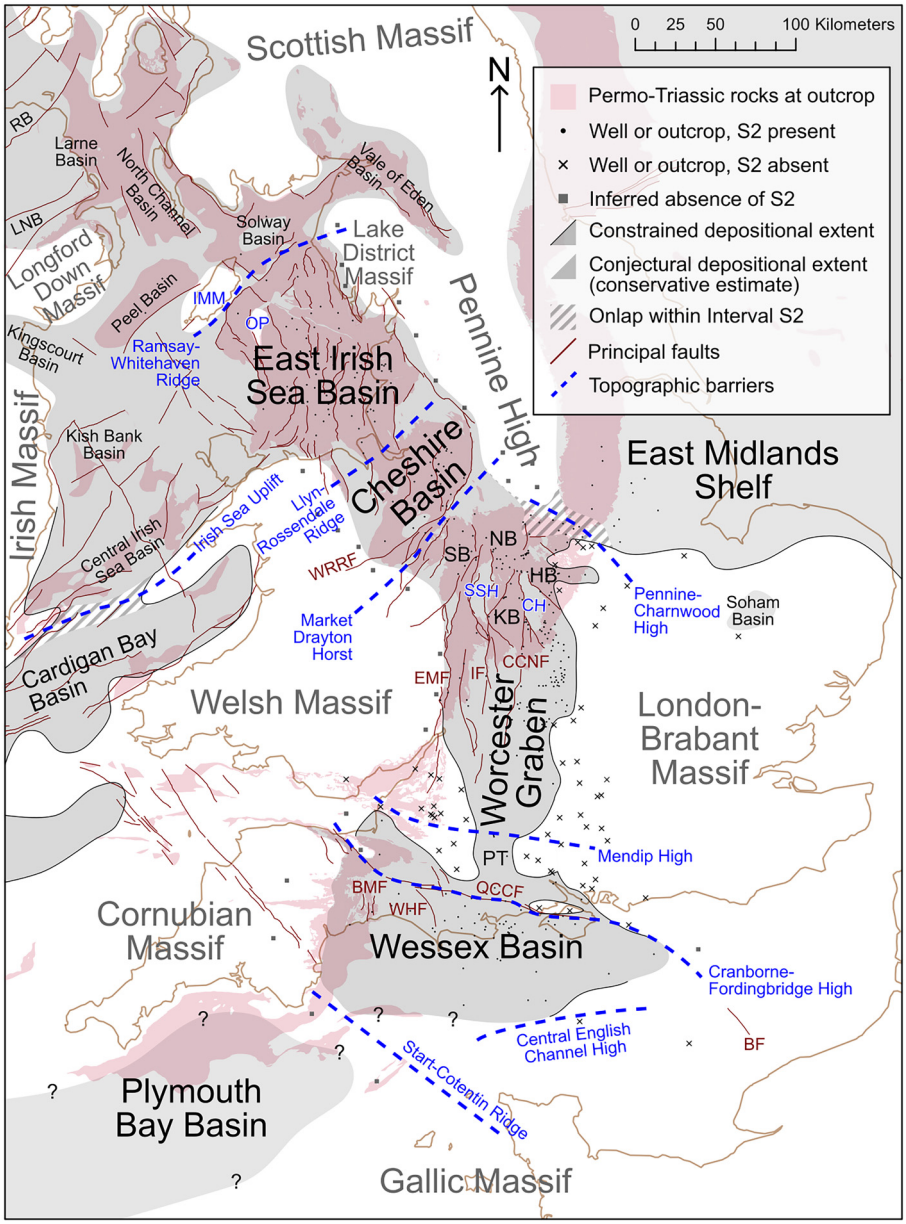


Fig. 5. Structural and palaeogeographical setting during Interval S2 (middle Triassic) in the British Isles. BF, Bray Fault; BMF, Beer–Musbury Fault; CH, Coventry Horst; CCNF, Clopton–Clapton–Northleach Fault; EMF, East Malvern Fault; HB, Hinkley Basin; IF, Inkerberrow Fault; IMM, Isle of Man Massif; KB, Knowle Basin; LNB, Lough Neagh Basin; NB, Needlewood Basin; OP, Ogham Platform; PT, Pewsey Trough; QCCF, Quantocks–Coker–Cranborne Fault; RB, Rathlin Basin; SB, Stafford Basin; SSH, South Staffordshire Horst; WHF, Wynford–Hooke Fault; WRRF, Wem–Red Rock Fault. Source: depositional extents outside geologically constrained areas from Jackson *et al.* (1995), Dunford *et al.* (2001), Simms (2009) and McKie (2017). Structures adapted from DiGRock250k (2013), DiGRock625k (2008) and Newell (2017*a*). Geological Map Data BGS © UKRI 2025.

sediment fairway mapping across the British Isles, subsequent volumetric calculations and the creation of a temporally defined sediment routing synthesis.

Palaeogeography and fairway extent

The mapped fairway of Interval S2 encompasses an area between the Wessex Basin in the south and the Central Irish Sea, Kish Bank and Peel basins in the north (Fig. 5). The fairway is surrounded by major upland areas, and smaller, mostly non-emergent structural highs that separate basins.

The southernmost depocentre is the Wessex Basin, bounded by the Central English Channel High to the south, the Start–Cotentin High to the SW, and the Cranborne-Fordingbridge High and Mendip High in the north (Fig. 5; Newell 2017*a*, *b*). Although the Wessex Basin was previously considered a basin produced largely by east–west-trending normal faults (e.g. Buchanan 1998; Butler 1998; Hawkes *et al.* 1998; Miliorizos and Ruffell 1998; Underhill and Stoneley 1998), recent evidence suggests that Triassic extension was largely controlled by an older set of north–south extensional faults, consistent with the Triassic stress regime and structural configuration of the Wessex Basin (Newell 2017*b*).

North of the Mendip High, the Wessex Basin passes into the Worcester Graben (Fig. 5). Although a connection between the two basins is critical in allowing long-distance, northwards sediment routing (Tyrrell *et al.* 2012; Newell 2017*a*), there has been no consensus on the connection's location through the Mendip High (Audley-Charles 1970; Wills 1970; Burley 1987; Warrington and Ivimey-Cook 1992; Newell 2017*a*; Burgess *et al.* 2025). We identify the point of connection in the area around the Shrewton 1 and Devizes 1 wells (Fig. 3), which penetrate *c.* 70 m of sandstone–siltstone facies, lithostratigraphically equivalent to the HSF. This area, termed the Pewsey Trough (PT; Fig. 5), had been a north–south-oriented, possibly fault-controlled depocentre since the Permian (Pullan and Donato 2022), and persisted as a deep, distinct depocentre in the late Triassic during MMG deposition (Newell 2024).

The Worcester Graben is a structurally controlled depocentre controlled by the East Malvern Fault, the Inkberrow Fault and the Clopton–Clapton–Northleach Fault (Fig. 5; Chadwick and Evans 1995; Newell 2017*a*), although the HSF also onlaps the pre-Permian basement to the west. There are four basins in the Midlands (Fig. 5), but they are grouped into a single 'Midlands Basins' province in our source-to-sink synthesis, owing to their connectivity and small size. The Midlands Basins are joined across the Market Drayton Horst to

Downloaded from https://www.lyellcollection.org by Imperial College of Science, Technology and Medicine on Jul 03, 2026

the Cheshire Basin. This is a half-graben basin primarily bounded by the Wem–Red Rock Fault in the SE (Fig. 5), and is separated from the EISB by the Llyn–Rossendale Ridge (Plant *et al.* 1999). The EISB contains numerous north–south faults that split the basin into sub-basins (Fig. 5; Jackson *et al.* 1995). Beyond the EISB, there are a series of smaller, fault-controlled depocentres, including the Solway, Larne, Peel, Kish Bank, Kingscourt and Central Irish Sea basins.

Lying to the east of the Pennine High is the East Midlands Shelf, a structurally simple, east-dipping ramp that forms the western edge of the Southern Permian Basin (Fig. 5; McKie 2017; Newell 2023). The HSF is absent on the East Midlands Shelf, which was probably never a depocentre for this unit. If the HSF had been deposited here, the strata would need to have been removed by erosion after the Mid-Triassic Unconformity, yet the resulting unconformity has never been found in any basin. In line with existing interpretations, the East Midlands Shelf was separated from the main fairway by an emergent Pennine–Charnwood high (Fig. 5; Warrington and Ivimey-Cook 1992; Ambrose *et al.* 2014; Newell 2017*a*, 2023), and became reconnected to the Midlands Basins only towards the end of this time interval (Ambrose *et al.* 2014; Jones *et al.* 2025).

Substantial upland areas served as sediment sources during the Triassic (e.g. Mange *et al.* 1999, 2007; Meadows 2006; Tyrrell *et al.* 2012; Morton *et al.* 2013, 2016; Burgess *et al.* 2025). These include the Gallic Massif to the south of the Wessex Basin (Fig. 5; *sensu* Sass *et al.* 2023). To the west, the fairway is bounded by the Cornubian, Welsh and Irish massifs, and to the east, by the Pennine High and London–Brabant Massif (Fig. 5). Smaller elevated regions are also present within the sedimentary fairway: the South Staffordshire Horst and Coventry Horst in the Midlands, and the Isle of Man Massif and the Ogham Platform in the EISB (Fig. 5).

Uncertainties in fairway extent

The southwesterly extent of the HSF in the Wessex Basin is largely unknown owing to limited offshore exploration. The southernmost wells that penetrate the HSF are 97/12–1 (Ainsworth and Riley 2010) and 97/24-1A (Fig. 3). The southern limit for the sediment fairway can be plausibly constrained to lie between the southernmost Permo-Triassic seabed outcrop (Fig. 5) and the modern-day Channel Islands and northern France, a recognized sediment source for the SSG (Morton *et al.* 2013). The fairway extent in the rest of the Wessex Basin and Worcester Graben is constrained by well data, with generally little postdepositional erosion (Fig. 5).

North of the Worcester Graben, Interval S2 is only partially preserved following post-depositional erosion. Although existing palaeogeographical interpretations all agree that Triassic units had a greater distribution in the past, the interpreted extent to which they were formerly distributed varies (Wills 1956, 1970; Audley-Charles 1970; Warrington and Ivimey-Cook 1992; Jackson *et al.* 1995; Dunford *et al.* 2001; Bourquin *et al.* 2011; McKie 2017).

Multiple lines of evidence can be used to constrain the original depositional extent of Interval S2. The absence of basin margin deposits analogous to those in the Wessex Basin and Worcester Graben (e.g. Smith and Edwards 1991; Barclay *et al.* 1997; Newell 2017*b*), palaeocurrents directed across palaeohighs (e.g. Thompson 1970*b*; Chisholm *et al.* 1988), outliers of SSG (Chisholm *et al.* 1988) and recycled Triassic detritus incorporated into younger deposits (Walsh *et al.* 1980, 2018) all indicate that the fairway extent used to be greater, and that the preserved distribution is primarily a reflection of where structurally controlled basins were deepest (Chadwick and Evans 1995). The most eroded area in the fairway encompasses the East Irish Sea, Peel, Kish Bank and Central Irish Sea basins (Fig. 5), which are interpreted to have formerly made up a contiguous 'Greater Irish Sea Basin' (*sensu* Dunford *et al.* 2001; Meadows 2006). However, we do not use this term, as sediment routing west of the EISB remains poorly understood. The original sediment fairway can also be inferred from the extent of Permian sedimentation, which occurred under the same extensional tectonic regime as the SSG. In the northern parts of the fairway, Interval S2 is likely to have overstepped, or at the very least equalled the distribution of Permian strata in the same way that it does in the Wessex Basin and Worcester Graben, where both Permian units and the SSG are fully preserved (Hamblin *et al.* 1992; Chadwick and Evans 1995). Our interpreted depositional boundaries (Fig. 5) are conservative estimates based on these lines of evidence.

Sediment isopachs

Isopach maps, created from compiled data constraints (Fig. 5), reconstruct deposited sediment thicknesses for Interval S2. Data coverage is sufficient to fully resolve sediment thicknesses between the Wessex Basin and the EISB, and partially resolve thicknesses in the Solway and Peel basins north of the Ramsay-Whitehaven Ridge (Fig. 6a). These maps accurately resolve the spatial and structural configuration of the sediment fairway for the first time. Deposition of all lithostratigraphic units occurs in deep, structurally controlled basins, with strata thinning over inter-basin palaeohighs (Fig. 6). The East Midlands Shelf (Fig. 5) was excluded from this volumetric analysis. As previously established, this was not a fluvial depocentre for the HSF, and stratigraphic markers coeval with those defining Interval S2 are absent (Fig. 4; Howard *et al.* 2008).

The HSF in the Wessex Basin is thickest towards the west, at 320 m. The HSF thins gradually towards the east, and towards the Gallic Massif in the south (Fig. 6b). Notably, thickness variations in the HSF are gradual (Fig. 6b), and appear to be controlled by only the oblique-slip Quantocks–Coker–Cranborne Fault System, which bounds the Cranborne–Fordingbridge High (Figs 5 and 6b; Newell 2017*b*). This shows that major west–east-trending extensional faults, which were active later in the Mesozoic (e.g. Buchanan 1998; Butler 1998; Hawkes *et al.* 1998; Miliorizos and Ruffell 1998; Underhill and Stoneley 1998) were inactive in the Triassic. In the Worcester Graben, the HSF thickens westwards towards the faulted basin margin, reaching a maximum of 400 m (Fig. 6b), which represents the greatest depositional thickness in the fairway. In the Midlands, the maximum thickness of the HSF is approximately 220 m in basin centres (Fig. 6b). The HSF in the Cheshire Basin is thickest in the SE, where thicknesses approach 210 m (Fig. 6b). Sediment thicknesses generally thin westwards towards the Llyn–Rossendale Ridge, and towards the southwestern basin margin. HSF thicknesses in the EISB are greatest at the basin centre, at 210 m (Fig. 6b), and decrease towards the basin margins.

The TSF is predominantly concentrated in the Cheshire Basin (Fig. 6c), where thicknesses reach 200 m in the SE. The TSF thins to the NW towards the southeastern EISB. Here, thicknesses do not exceed 100 m. To the south, the TSF is widely distributed but thin (<50 m) in the Midlands, East Midlands Shelf and the Worcester Graben, locally reaching 60 m thick in the hanging wall of the East Malvern Fault.

The lower SMF (below the Preesall and Northwich Halites) (Fig. 6d) is up to 410 m thick in the northeastern Cheshire Basin, although it is generally 200–400 m thick elsewhere in the basin. In the EISB, the SMF gradually thickens towards the NW part of the basin, where the unit reaches thicknesses of 900 m (Fig. 6d). The SMF thins towards the Ramsay–Whitehaven Ridge, and the basin margin in the west.

The Northwich Halite in the Cheshire Basin reaches a maximum thickness of 230 m (Fig. 6e), and is thickest along a NW–SE axis through the centre of the basin, thinning out towards the basin margins. The Preesall Halite is 570 m thick in the centre of the EISB (Fig. 6e), and is thickest along a north–south axis at the basin centre. Both the extent and the thickness of the Preesall Halite are reduced

Downloaded from https://www.lyellcollection.org by Imperial College of Science, Technology and Medicine on Jul 03, 2026

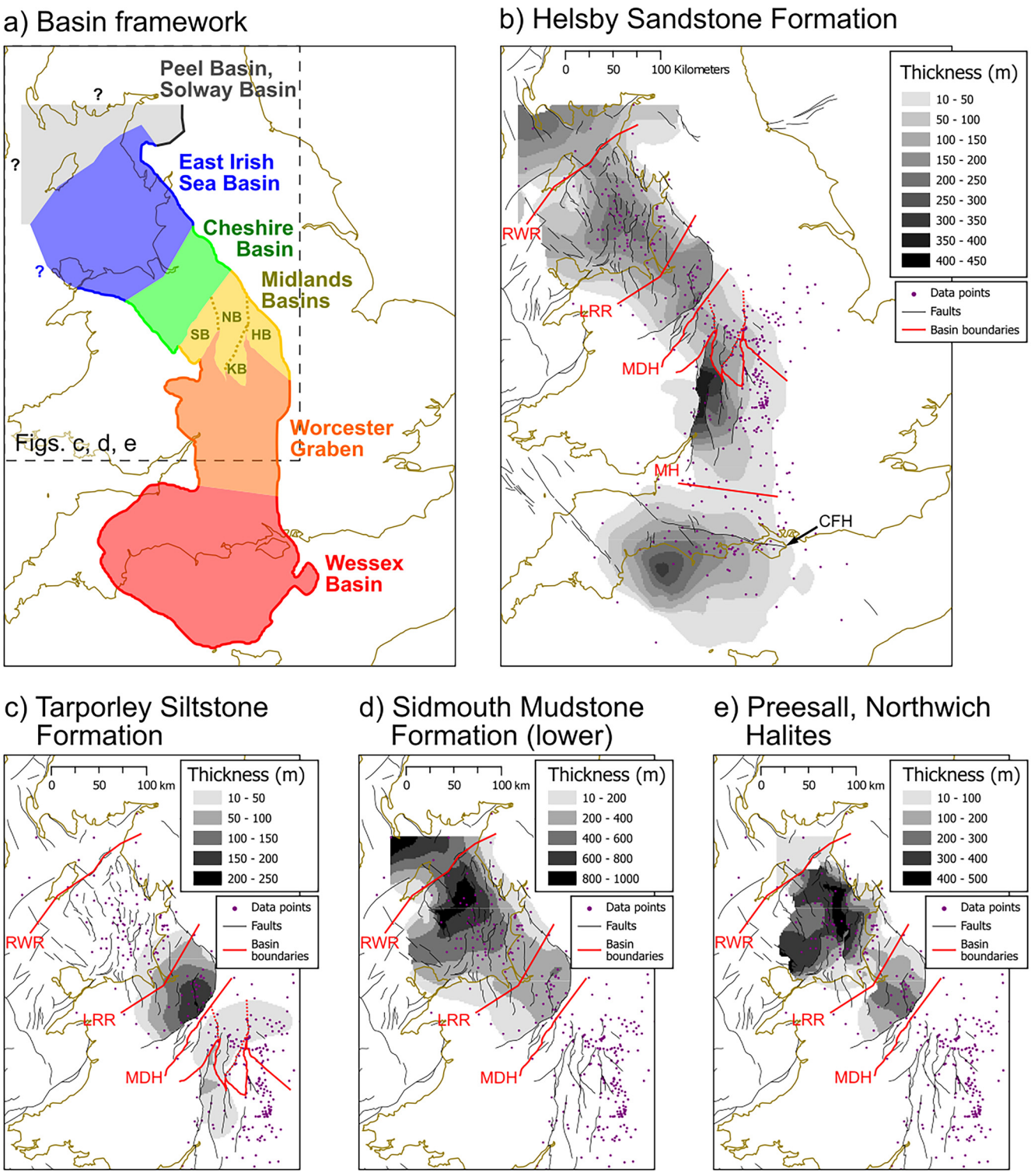


Fig. 6. (**a**) Basin configuration for isopach maps of the lithostratigraphic units of Interval S2. Isopach maps for the (**b**) Helsby Sandstone Formation (**c**) Tarporley Siltstone Formation (MMG), (**d**) Sidmouth Mudstone Formation (below but excluding the Preesall and Northwich Halites) and (**e**) Preesall and Northwich Halites. SB, Stafford Basin; NB, Needlewood Basin; HB, Hinkley Basin; KB, Knowle Basin; CFH, Cranborne–Fordingbridge High; MH, Mendip High; MDH, Market Drayton Horst; LRR, Llyn–Rossendale Ridge; RWR, Ramsay–Whitehaven Ridge.

over the Llyn–Rossendale Ridge, where thicknesses do not exceed 200 m.

Sediment porosity and facies

The calculated proportion of aeolian and fluvial deposits reflects the distribution of sediment at the time of deposition, and provides insight into the distribution of aeolian and fluvial processes operating within the HSF fairway. It should be noted that this figure cannot directly represent the extent of fluvial–aeolian sediment reworking, nor the ultimate provenance of the sediments. These aspects require further sedimentological and petrographic data to discern, and are discussed below as part of the basin-by-basin synthesis of sediment routing.

For the HSF, the proportion of fluvial deposits in the EISB is 64%, and was estimated by averaging areas covered by mapped seismic facies (figs 8 and 9 of Meadows and Beach 1993*b*). The proportion of fluvial deposits in the Cheshire Basin is 71%, and was

Downloaded from https://www.lyellcollection.org by Imperial College of Science, Technology and Medicine on Jul 03, 2026

estimated from vertical facies successions from borehole logs (figs 6 and 7 of Thompson 1970*a*). In the Midlands and Worcester Graben, the composition of the HSF is assumed to be 100% fluvial, as no widespread aeolian facies have been documented in outcrop, core or wireline log data (Ambrose *et al*. 2014). In the Wessex basin, the first-order proportion of fluvial deposits is estimated at 90% and is consistent in both the western and central areas (McKie *et al*. 1997; Newell 2017*b*).

Sediment volumes

The solid rock (porosity removed) sediment volume for Interval S2 is 15 600 km^3 (Fig. 7, with further data in Supplementary material 3). Of this volume, 5590 km^3 (36%) is represented by the HSF of the SSG. The remaining 10 000 km^3 (64%) is represented by the MMG. Within the MMG, 613 km^3 is in the TSF, 6190 km^3 in the lower SMF and 3210 km^3 in the Preesall and Northwich Halites; these lithostratigraphic units comprise 4, 40 and 20% of the total sediment volume of Interval S2, respectively.

By volume, the EISB is the largest basin, with a total sediment volume of 9750 km^3, representing 62% of the total volume of Interval S2 (Fig. 7). However, the HSF forms only 1820 km^3 (19%) of the EISB's sediment volume, and only 1160 km^3 (12%) is composed of HSF fluvial deposits. The Cheshire Basin is the second largest depocentre, with a total sediment volume of 2500 km^3. The HSF forms 533 km^3 (21%) of the Cheshire Basin's total volume, of which 379 km^3 (15%) is fluvial deposits. The Wessex Basin is third largest depocentre, with a total sediment volume of 1870 km^3. Interval S2 is composed of only the HSF here, with 1690 km^3 of fluvial deposit volume. The Worcester Graben has a total sediment volume of 1090 km^3. Sediment volumes here are dominated by the entirely fluvial HSF, at 1030 km^3 (95%), with the remainder of this volume (54.5 km^3, 5%) comprising the TSF. The Midlands Basins are collectively the smallest depocentre, with a total sediment volume of 386 km^3. Again, this volume is dominated by the entirely fluvial HSF, at 335 km^3 (87%), with 51.7 km^3 (13%) being the TSF. Overall, the largest volume of HSF occurs in the Wessex Basin, followed by the EISB, the Worcester Graben, the Cheshire Basin and then the Midlands basins (Fig. 7).

When sediment volumes are integrated with the well-constrained chronostratigraphy in the EISB and Wessex Basin (Fig. 4), solid rock sediment accumulation rates can be calculated. In the EISB, Interval S2 has a total duration of 5 Myr: 2.5 Myr for the HSF and 2.5 Myr for the lower MMG (TSF, SMF and Preesall Halite). In the Wessex Basin, Interval S2 has a duration of 6.9 Myr. For the EISB, sediment accumulation rates increase fourfold from 726 km^3 Ma^{-1} in the HSF to 3170 km^3 Ma^{-1} in the lower MMG. The overall accumulation rate across Interval S2 in the EISB is 1950 km^3 Ma^{-1}. In the Wessex Basin, the sediment accumulation rate within Interval S2 is 271 km^3 Ma^{-1}.

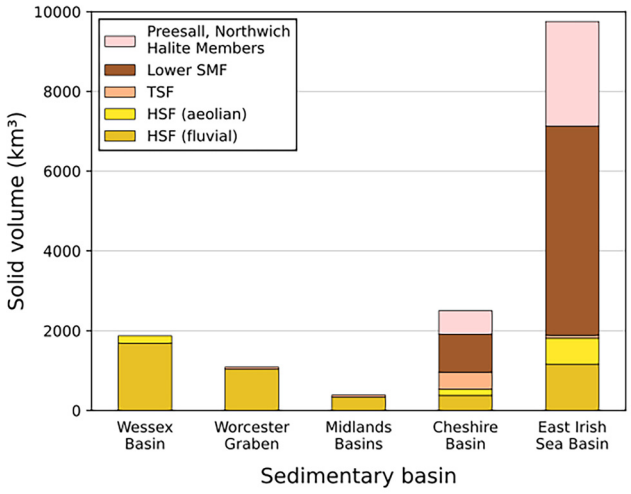


Fig. 7. Solid rock (porosity removed) sediment volumes for the basins within Interval S2 (Fig. 2), arranged down-system (south to north) between the Wessex Basin and the EISB (Fig. 6). Volumes are divided by respective lithostratigraphic units, and within the Helsby Sandstone Formation (HSF) by aeolian and fluvial deposits. TSF, Tarporley Siltstone Formation; SMF, Sidmouth Mudstone Formation.

Errors and uncertainties in sediment volume

Uncertainties in the original fairway extent cause uncertainties in calculated sediment volumes. The greatest uncertainty in fairway extent occurs in the southwestern part of the Wessex Basin, where there are very few constraints on the thickness and distribution of the HSF (Fig. 3). North of the Midlands (Fig. 6a), uncertainties in fairway extent are caused by post-depositional erosion. This uncertainty is reduced by the fact that basin centres are fully preserved and well constrained, with only the former basin margins, where Interval S2 was thinnest, being eroded. Furthermore, as the boundaries of the sediment fairway are drawn from conservative estimates (Fig. 5), the resulting isopach maps and sediment volumes are also conservative estimates.

Uncertainties in defining lithostratigraphic boundaries are low, as for most units, lithologies and wireline log responses are distinct (e.g. Meadows 2006; Ambrose *et al*. 2014; Newell 2017*a*; Chedburn *et al*. 2022). More uncertainty occurs in areas where the TSF is gradational between the HSF and the SMF. However, the impact of this uncertainty at the fairway scale is small, as the TSF is the volumetrically smallest unit in Interval S2 (Fig. 7).

Uncertainty in rock porosity is generally low in the SSG, as porosity is well characterized from a large dataset compiled across the sediment fairway (Table 2; Bowman *et al*. 1993; Newell and Shariatipour 2016; Medici *et al*. 2019*a*). Uncertainties in the MMG are higher, as far fewer measurements of porosity are available (Parkes *et al*. 2021). However, owing to the limited range of porosities in mudstones (<20%; AlNajdi and Worden 2023), the impact of porosity on sediment volume is limited compared with the other uncertainties discussed.

The classification of fluvial and aeolian deposits in the HSF in the Cheshire Basin and EISB represents a further uncertainty. Although there is good spatial coverage of basin-scale sedimentology, criteria used to recognize aeolian, fluvial and fluvial–aeolian successions differ between these basins (Thompson 1970*a*; Meadows and Beach 1993*b*). Our calculated fluvial and aeolian deposit volumes, which are derived from these facies distributions, represent a first-order estimation of the facies distribution within the sediment fairway.

Bulk sandstone mineralogy in the HSF

Data for bulk sandstone mineralogy in the HSF are outlined in Table 3, and are classified by study, point counting method and depocentre. Overall, there is a notable difference in bulk sandstone mineralogy between the Wessex Basin in the southern part of the sediment fairway and the Midlands basins, Cheshire Basin and EISB (Fig. 8a). Although there is an absence of data in the Worcester Graben, sandstones are clearly more feldspathic in the southern part of the fairway than the north (Fig. 8b; see Supplementary material 4 for full dataset).

By the Gazzi–Dickinson method of point counting, quartz and feldspar are the dominant mineralogical components in the HSF, although proportions change substantially between basins. In the Wessex Basin, bulk sandstone mineralogy appears similar in both the eastern and western basin, with quartz, feldspar and lithic

Downloaded from https://www.lyellcollection.org by Imperial College of Science, Technology and Medicine on Jul 03, 2026

Table 3. Summary statistics for petrographic data within the Helsby Sandstone Formation (HSF), grouped by study, by point count method (Augustsson 2021) and by basin

	Point count method	Wessex Basin (W)	Wessex Basin (E)	Worcester Graben	Midlands Basins	Cheshire Basin	East Irish Sea Basin
De Sainz Simpson (2022)	Gazzi–Dickinson					41	44
Scorgie *et al.* (2021)	Traditional						12
Meadows (2004)	Traditional					10	121
Svendsen and Hartley (2001)	Gazzi–Dickinson	23					
Chisholm *et al.* (1988)	Unclassified				1		
Burley (1987)	Traditional	9	11			11	18
Knox *et al.* (1984)	Gazzi–Dickinson		14				
Ali (1982)	Unclassified				5		

contents of 50–70, 20–50 and 0–20%, respectively (Fig. 8b; Knox *et al.* 1984; Svendsen and Hartley 2001). Although there are no quantified petrographic data for the central part of the Wessex Basin (Fig. 8a), its bulk mineralogy appears comparable with the eastern and western Wessex Basin (Rhys 1982; Bath *et al.* 1987). To the north, the HSF appears to have a similar bulk mineralogy in both the Cheshire Basin and EISB, with a quartz content of 80–95%, a feldspar content of 0–15% and a lithic content of 0–10% (Fig. 8b; De Sainz Simpson 2022). Furthermore, fluvial and aeolian sandstone facies in the Cheshire Basin and EISB appear to have a similar bulk mineralogy.

By the Indiana method of point counting, resultant proportions of quartz, feldspar and lithic fragments are more variable, although again, mineralogical proportions vary between basins. In the Wessex Basin, the HSF largely has a quartz content of 40–70%, a feldspar content of 15–50% and lithic content of 10–50% (Fig. 8b; Burley 1987). In the Cheshire Basin and EISB, bulk sandstone compositions are similar, with quartz, feldspar and lithic contents of 50–90, 0–25 and 5–40%, respectively (Fig. 8b; Burley 1987; Meadows 2004; Scorgie *et al.* 2021). In the Cheshire Basin, there appears to be a difference in bulk mineralogy between fluvial and aeolian facies, with aeolian sandstones ($n = 4$) being more quartz-rich than fluvial sandstones ($n = 58$). In the EISB, fluvial and aeolian facies appear to have a similar bulk mineralogy.

Sediment mineralogical data appear consistent in the Midlands, despite the point counting method being unclassified. The quartz content of sandstones is 80–90%, the feldspar content is 5–15% and the lithic content is 2–10% (Fig. 8b; Ali 1982; Chisholm *et al.* 1988).

Diagenesis and its impact on bulk sandstone mineralogy

Diagenetic alteration of unstable detrital grains also contributes to uncertainties in reconstructing original bulk sandstone mineralogy. Lithic fragments and feldspars are ubiquitously altered in the HSF across all basins, as shown by by grain dissolution textures, skeletal grains and the presence of authigenic clays and feldspars (e.g. Ali and Turner 1982; Burley 1984; Knox *et al.* 1984; Bushell 1986; Strong and Milodowski 1987; Greenwood and Habesch 1997; Plant *et al.* 1999; Scorgie *et al.* 2021). Grain dissolution porosity is measured at 7% in Devon in the western Wessex Basin, 8% in the Marchwood 1 borehole in the eastern Wessex Basin and up to 7% in the EISB margin (Burley 1984).

On the fairway scale, the maximum burial depth for the HSF can be used to approximate the maximum effects of diagenesis in each basin. Burial histories (Fig. 9) are derived from apatite fission-track analysis and vitrinite reflectance (Carter *et al.* 1995; Mikkelsen and Floodpage 1997; Bray *et al.* 1998; Gent 2016; Pharaoh *et al.* 2019). Selected wells are located away from basin margins, and so probably represent maximum burial depths for each basin. The burial depth for the HSF at the Wytch Farm oilfield in the Wessex Basin is 3.5 km (Bray *et al.* 1998). The SSG in the Midlands Basins reached a palaeotemperature of 75 ± 10°C between 150 and 70 Ma (Carter *et al.* 1995). Assuming a geothermal gradient of 30°C km^{-1}, this implies a burial depth of 2.5 ± 0.3 km (Fig. 9b). The HSF in the Knutsford 1 well in the Cheshire Basin reached a burial depth of 2.9 km (Fig. 9b; Mikkelsen and Floodpage 1997), and 1.8 km for well 110/7b-6 in the EISB (Fig. 9b; Gent 2016; Pharaoh *et al.* 2019). This implies that the HSF across Great Britain reached comparable maximum burial depths (*c.* 3 km), except in the EISB, which was buried to shallower depths (*c.* 2 km). This in turn suggests that the maximum impact of diagenesis is similar in all basins except for the ESIB, which may have experienced less extreme diagenetic alteration.

These figures indicate that HSF sandstones were originally more lithic- and feldspar-rich, with a modest amount (<10% total rock volume) of grains removed during burial diagenesis. Data points in Figure 8b cannot be translated uniformly to remove diagenetic effects, as burial depths and diagenetic histories differ for data collected at basin margins and palaeohighs compared with deeper basin centres (Bray *et al.* 1998; Green *et al.* 2001; Scorgie *et al.* 2021). However, the variance of bulk sandstone detrital mineralogy both within and between basins (Fig. 8b) is substantially greater than any compositional variations expected from diagenesis. This in turn indicates that spatial variations in sandstone composition are a primarily depositional signal, and so can be used to interpret sediment routing within the fairway.

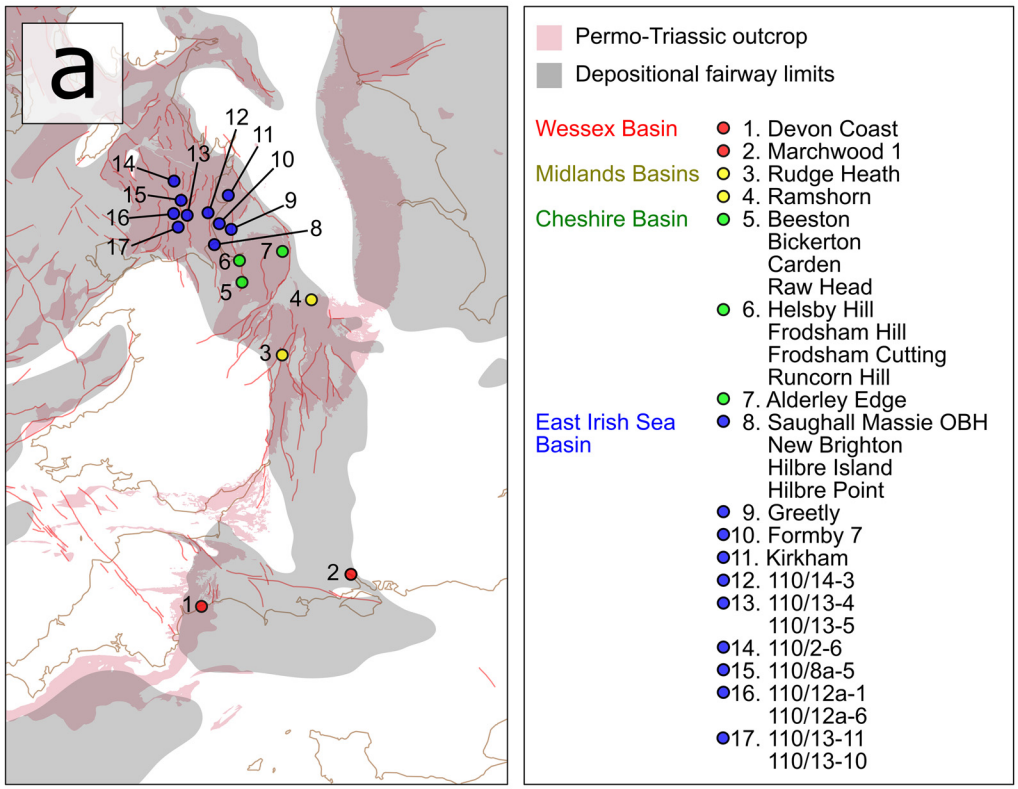
Fairway sediment routing

Overall, our source-to-sink synthesis suggests that Interval S2 was deposited by a single, continuous fluvial system, as shown by consistently north- and NW-directed palaeocurrents and an overall decrease in grain size along the sediment fairway (Fig. 10a and b). The connectivity of sediment routing is also strongly supported by our synthesis of quantitative provenance analysis (Plant *et al.* 1999; Tyrrell *et al.* 2012). Our synthesis also resolves the presence of secondary sediment inputs and fluvial–aeolian interactions, and provides insight into sediment routing beyond the EISB and across the transition between the SSG and MMG (i.e. the distal segments of the Sherwood-2 River System). A more detailed overview of sediment routing in the Wessex, Cheshire and East Irish Sea basins, as well as the SSG–MMG transition, is presented in the Supplementary Material to honour the breadth and depth of published information available.

Sediment routing within the HSF

In the Wessex Basin, quantitative provenance analysis indicates the Sherwood-2 River System operated as a series of at least three north-flowing tributaries (Fig. 10a; Morton *et al.* 2016). The HSF is dominated by material with a Variscan–Cadomian provenance,

Downloaded from https://www.lyellcollection.org by Imperial College of Science, Technology and Medicine on Jul 03, 2026



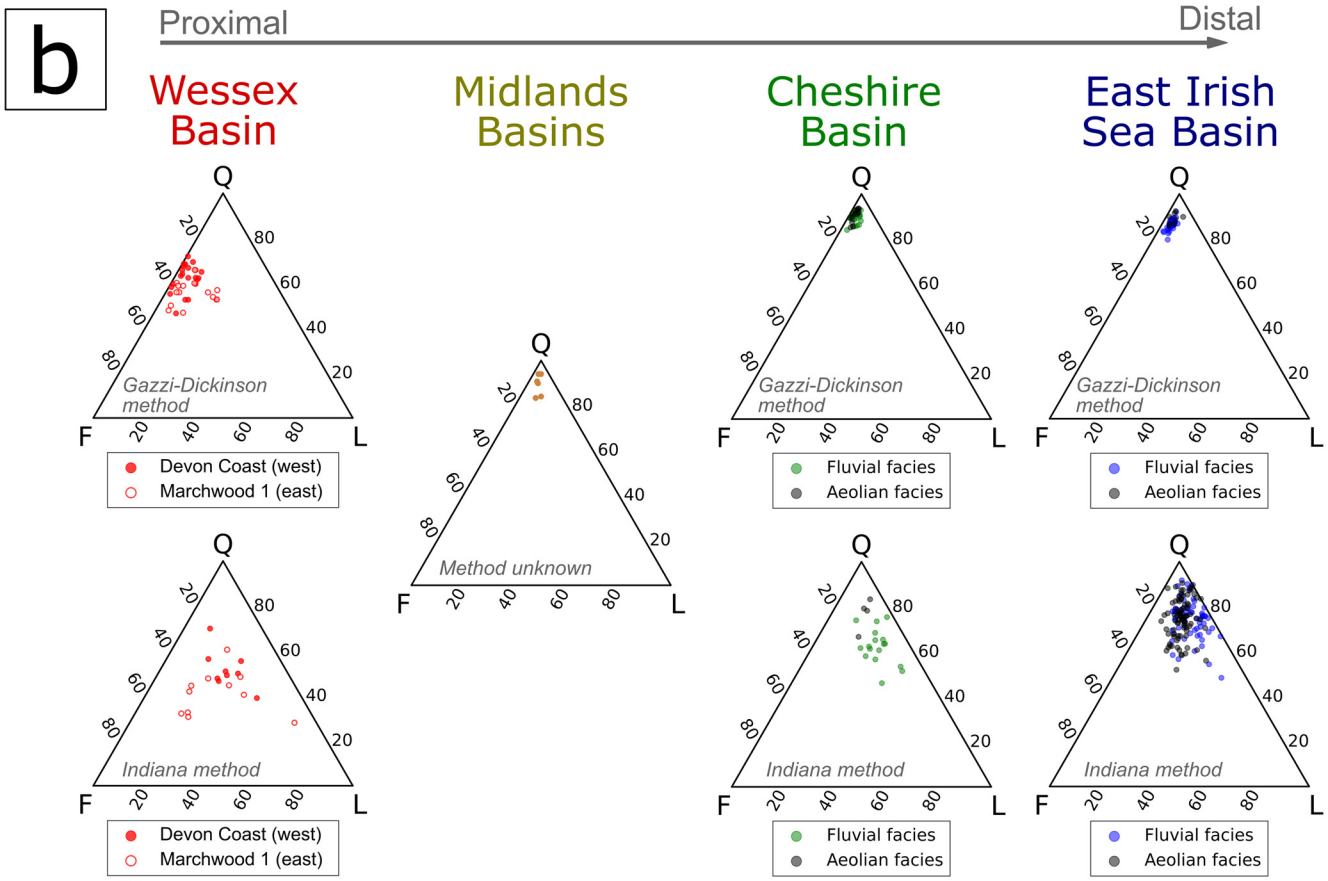


Fig. 8. (**a**) Map showing localities within the Helsby Sandstone Formation (HSF) where sandstone bulk petrographic data have been collected, divided by sedimentary basin. (**b**) Sandstone QFL plots for each basin area in the HSF, divided by point count method. Bulk mineralogical data are also divided between fluvial and aeolian deposits in the Cheshire Basin and EISB. Source: (a) Ali (1982), Knox *et al.* (1984), Burley (1987), Chisholm *et al.* (1988), Meadows (2004), Scorgie *et al.* (2021) and De Sainz Simpson (2022). Geological Map Data BGS © UKRI 2025; (b) diagrams plotted using Ternary-Diagram (Yu9824 2021).

Downloaded from https://www.lyellcollection.org by Imperial College of Science, Technology and Medicine on Jul 03, 2026

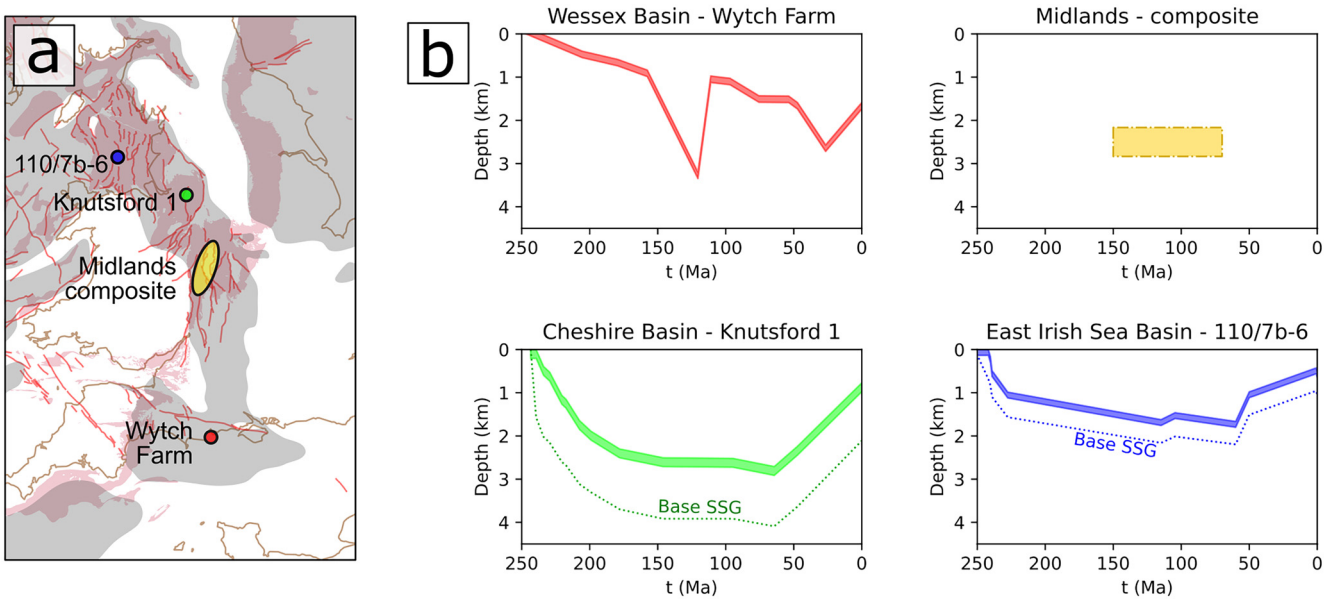


Fig. 9. (**a**) Map showing selected localities where burial histories for the Helsby Sandstone Formation (HSF) are reconstructed from vitrinite reflectance and apatite fission-track analysis. (**b**) Representative burial histories for each basin, taken at the Wytch Farm oilfield for the Wessex Basin, a composite of wells in the western part of the Midlands Basins, well Knutsford 1 in the Cheshire Basin and well 110/7b-6 in the EISB. Source: (a) Geological Map Data BGS © UKRI 2025. (b) Wytch Farm oilfield from Bray *et al.* (1998), wells in the western part of the Midlands Basins from Carter *et al.* (1995), well Knutsford 1 in the Cheshire Basin from Mikkelsen and Floodpage (1997) and well 110/7b-6 in the EISB from Gent (2016)).

sourced from the basement units of the Gallic Massif (Tyrrell *et al.* 2012; Morton *et al.* 2013, 2016). This is supplemented by material sourced from the granites of the Cornubian Massif (Smith and Edwards 1991) and recycled Devonian sediment from the London–Brabant Massif (Morton *et al.* 2016). All tributaries probably coalesced south of the Pewsey Trough and flowed nothwards as a single trunk river into the Worcester Graben (Fig. 10a).

In the Worcester Graben, the main axis of sediment routing was to the north (Fig. 10a; Old *et al.* 1991). Although the presence of extraformational clasts in the HSF suggests proximal sediment inputs (Barclay *et al.* 1997; Old *et al.* 1991), there are no contemporary studies of sediment provenance or petrography in the Worcester Graben, and the details of sediment routing here are largely unknown.

In the Midlands Basins, recorded palaeocurrent azimuths suggest that the primary axis of sediment routing was northwards (Fig. 10a; Old *et al.* 1987, 1991; Chisholm *et al.* 1988). Multiple sediment inputs from the Welsh and London–Brabant massifs were proposed by Audley-Charles (1970), based on observed clast compositions in the HSF (Fig. 10a). The pronounced difference in HSF bulk sandstone composition between the Wessex Basin and the Midlands Basins (Fig. 8b) suggests that substantial dilution of Variscan-derived material by sediments from other source areas had already occurred before the Sherwood-2 River System reached the Midlands Basins (Plant *et al.* 1999; Morton *et al.* 2013). However, bulk sandstone mineralogical data for the Midlands Basins are limited (Fig. 8b), and thus the mineralogical diversity of the HSF here may not be fully captured. The CHF in the Midlands appears to have a substantial lithic component (Indiana method; Burley 1987) which could also be present in the HSF.

During much of Interval S2, an emergent Pennine–Charnwood Ridge disconnected the Sherwood-2 River System from the East Midlands Shelf. Accordingly, the East Midlands Shelf was devoid of large-scale fluvial activity, and was instead a low-energy coastal plain where the MMG was deposited (Jones *et al.* 2025). Reconnection between the Midlands and the East Midlands Shelf occurred during the latter stages of Interval S2 during deposition of the TSF (Fig. 10b).

In the Cheshire Basin, palaeocurrents suggest that the main axis of fluvial transport was towards the NW (Fig. 10a; Thompson 1970*b*; Plant *et al.* 1999; Mountney and Thompson 2002; De Sainz Simpson 2022; Cosgrove *et al.* 2025). This was accompanied by an input of fluvial sediment from the Welsh Massif (Plant *et al.* 1999) (Fig. 10a). A further, well-documented component of aeolian activity is associated with the fluvial system. Palaeowinds originated from the east, and aeolian sediment was sourced from the Pennine High (Fig. 10a; Thompson 1970*b*; Rees and Wilson 1998; Mountney and Thompson 2002; De Sainz Simpson 2022; Cosgrove *et al.* 2025). The proportion of fluvial and aeolian deposits is highly variable both spatially and temporally (e.g. Burley 1987; Cosgrove *et al.* 2025), and their distribution probaby had underlying climate and subsidence controls, which in turn controlled sediment flux, accommodation generation and water table level (Newell 2017*a*; Cosgrove *et al.* 2025). In spite of this variability, a throughgoing, NW-flowing fluvial system was maintained, as widespread, perennial fluvial activity occurred downsystem in the EISB (Meadows and Beach 1993*a*, *b*; Meadows 2006).

In the EISB, the Sherwood-2 River System entered the basin in the south, and then turned west (Cowan 1993; Herries and Cowan 1997; Plant *et al.* 1999; Dunford *et al.* 2001; Meadows 2006; Marsh *et al.* 2022). Here, Mange *et al.* (1999, 2007) also identified a sediment input from the Welsh Massif (Fig. 10a), although this signal may have propagated from the Cheshire Basin. There was also an aeolian sediment source from the Pennine High to the east (Fig. 10a; Meadows and Beach 1993*a*; Jones and Ambrose 1994; Meadows 2006; Scorgie *et al.* 2021; Marsh *et al.* 2022). There was probably considerable aeolian reworking of fluvial sediments in the EISB prior to deposition: monocrystalline feldspars within both fluvial and aeolian facies have a provenance signal suggesting a Gallic Massif source (Tyrrell *et al.* 2012). There is no systematic variation in mineralogy between facies (Fig. 8b), suggesting that these feldspars were also well mixed in the basin. The provenance of the lithic fragments, which are composed primarily of quartz and feldspar and are also present in the Cheshire Basin (Fig. 8b), is currently unknown. More marginal localities of the EISB are 100% aeolian (Jones and Ambrose 1994; Medici *et al.* 2019*a*), whereas

Downloaded from https://www.lyellcollection.org by Imperial College of Science, Technology and Medicine on Jul 03, 2026

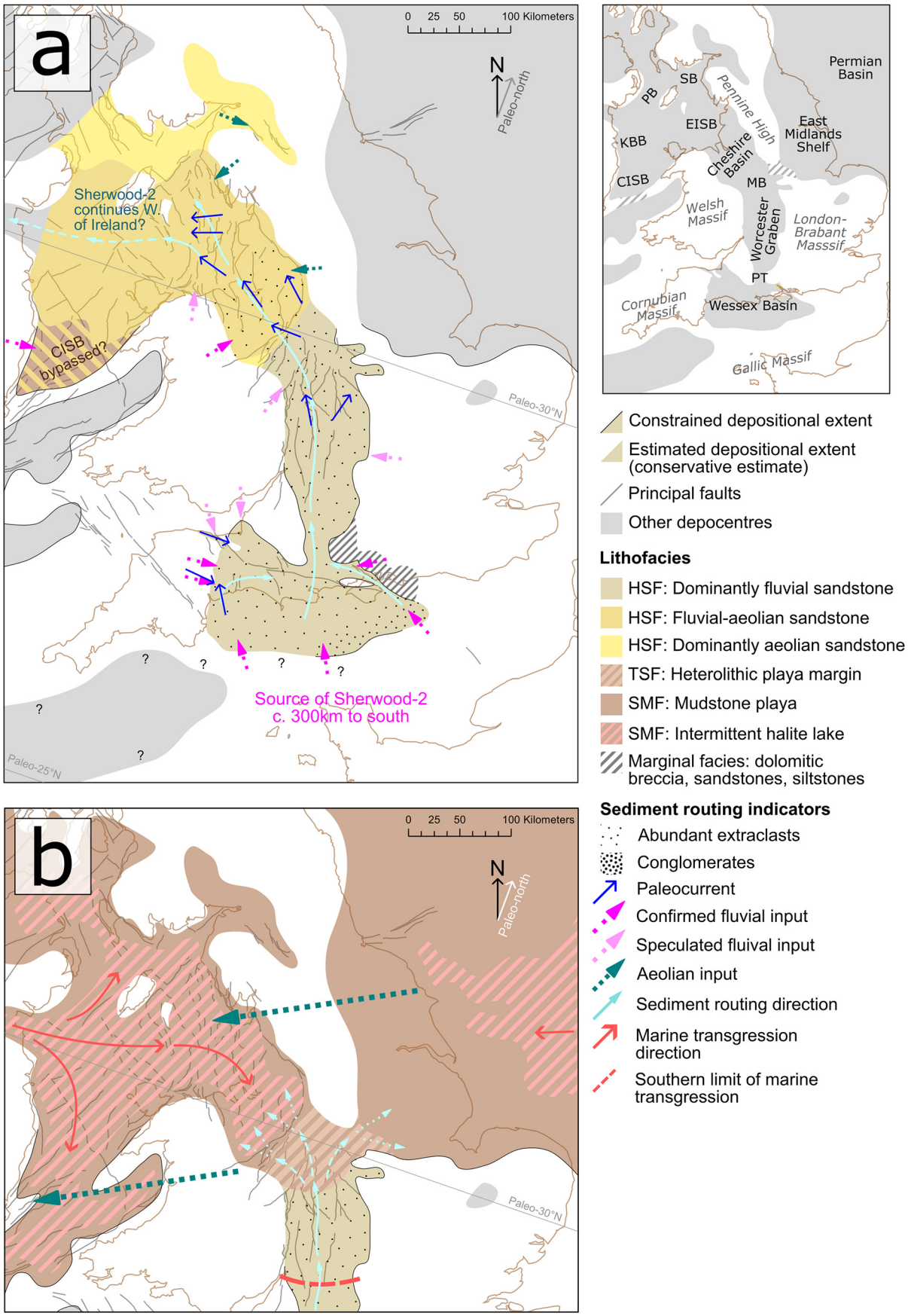


Fig. 10. Depositional environments (**a**) for the base of Interval S2 (Fig. 4, Helsby Sandstone Formation, HSF), and (**b**) the top of Interval S2 in the northern portion of the fairway (Fig. 4, HSF, Tarporley Siltstone Formation (TSF), lower Sidmouth Mudstone Formation (SMF). Also depicted are confirmed and speculated sediment inputs, representative palaeocurrent and first-order grain-size changes. Palaeogeography and sediment fairway follows Figure 5 and references therein. EISB, East Irish Sea Basin; CISB, Central Irish Sea Basin; KBB, Kish Bank Basin; MB, Midlands basins; PB, Peel Basin; PT, Pewsey Trough; SB, Solway Basin. Source: (a, b) confirmed and speculated sediment inputs from Wills (1956, 1976), Audley-Charles (1970), Smith and Edwards (1991), Jones and Ambrose (1994), Mountney and Thompson (2002), Tyrrell *et al.* (2012), Morton *et al.* (2013, 2016) and Marsh *et al.* (2022);

Downloaded from https://www.lyellcollection.org by Imperial College of Science, Technology and Medicine on Jul 03, 2026

representative palaeocurrent measurements from Thompson (1970*b*), Old *et al*. (1987, 1991), Chisholm *et al*. (1988), Smith and Edwards (1991), Herries and Cowan (1997), Edwards (1999) and Newell 2017*b*). Palaeo-north and palaeolatitude from Dercourt *et al*. (2000).

major fluvial activity is maintained in the basin centre, with aeolian facies only forming 5–10% of the rock volume in the Morecambe Ggas Field (Cowan 1993). In more detail, spatial partitioning of fluvial and aeolian deposits in the basin may have followed structurally controlled highs and lows (Meadows and Beach 1993*b*).

After the EISB, the Sherwood-2 River System flowed further west to the Kish Bank, Peel and Central Irish Sea basins. These basins formerly formed a contiguous depocentre with the EISB (Fig. 10a; Dunford *et al*. 2001; Meadows 2006; Marsh *et al*. 2022). The sedimentology of the HSF in these basins is poorly characterized relative to the rest of the HSF fairway, a problem exacerbated by the severe degree of post-Triassic erosion in the area. All basins contain a mix of fluvial and aeolian sandstone facies (Naylor *et al*. 1993; Newman 1999; Dunford *et al*. 2001; Floodpage *et al*. 2001).

During the early stages of Interval S2, the Irish Sea area was unlikely to have been the ultimate terminus of the Sherwood-2 River System, as there is no indication of an endorheic terminal splay system here (e.g. McKie 2011, 2014; Gibson-Poole *et al*. 2026). Topographic barriers and an absence of fluvial facies within strata equivalent to Interval S2 indicate that the Sherwood-2 River System did not flow north towards the Solway and North Channel basins (Fig. 10a; Marsh *et al*. 2022) or south into the Celtic Sea Trough (Fig. 10a; Dunford *et al*. 2001). It is most likely that the Sherwood-2 River System therefore flowed west via the Kingscourt Basin, possibly draining externally towards the shallow-marine Porcupine Basin, west of Ireland (Croker and Shannon 1987).

Sediment routing across the SSG–MMG transition

The onset of MMG deposition is diachronous (Fig. 4), and coincides with the regional Muschelkalk marine transgression and a climatic aridification (Greenwood and Habesch 1997; Thompson and Meadows 1997; McKie 2014; Newell 2017*a*). Within the lower MMG, marine flooding was brief, shallow, but regular, as is well shown by isotope geochemistry, sedimentology and palaeontology (e.g. Greenwood and Habesch 1997; Old *et al*. 1991; Barclay *et al*. 1997; Thompson and Meadows 1997; Evans *et al*. 2011; Warrington and Pollard 2021). These transgressions probably originated from the marine domain west of Ireland (Croker and Shannon 1987) and combined with aridification caused a southwards backstepping of fluvial activity and an ingress of halite lake and playa facies initially into the EISB, and then into the Cheshire Basin, Midlands basins and Worcester Graben by the end of the Anisian (Figs 4 and 10b).

In the EISB, there is a sharp transition from the aeolian and sabkha deposits of the HSF into the playa lake deposits of the SMF (Fig. 4; Thompson and Meadows 1997; Meadows 2006). In the Cheshire Basin, the aeolian-dominated upper HSF changes into the playa margin deposits of the TSF (Figs 4 and 6c; Burley 1987; Mikkelsen and Floodpage 1997; Scorgie *et al*. 2021; De Sainz Simpson 2022). In the Midlands Basins and Worcester Graben, the fluvial deposits of the HSF change into fluvial, playa margin and marginal marine deposits of the TSF (e.g. Warrington 1970*a*, *b*; Charsley 1982; Old *et al*. 1991; Barclay *et al*. 1997; Warrington and Pollard 2021; Jones *et al*. 2025), although these latter successions are thin and impersistent (Fig. 6c). The Worcester Graben represents the southern limit of marginal marine deposits in the TSF (Fig. 4). In the Wessex Basin, the uppermost HSF is composed of ephemeral lacustrine and sandflat deposits in the basin centre (McKie *et al*. 1997) and is fluvial in the west (Newell 2017*b*). Both areas then show a change into the arid playa lake mudstones of the SMF (Fig. 4). Although sand-grade sedimentation ceased during the deposition of the MMG, the dominance of terrestrial and shallow subaqueous depositional environments in this unit (Arthurton 1980; Wilson 1993) implies that sediment fluxes remained sufficient to fill basins. The EISB was filled despite the previously calculated fourfold increase in sediment accumulation rate across the SSG–MMG boundary. A general increase in accommodation generation through time, owing to varying tectonic subsidence rate (Newell 2017*a*), may have contributed to the southwards retreat of sand-grade deposition (e.g. Paola and Martin 2012; Reynolds 2024). Further insight into the role of active faulting in controlling stratigraphic architecture is possible only with decompaction and better chronostratigraphic constraints.

During the later stages of Interval S2, the assemblage of evaporitic playa lake, playa margin and intercalated fluvial–aeolian deposits in the SMF, TSF and HSF (Fig. 4) corresponds well to a terminal splay depositional model (e.g. Lang *et al*. 2004; McKie 2011, 2014). Incoming fluvial systems were dispersed at the playa margin. Fluvial activity became increasingly ephemeral and unconfined, and declined rapidly towards the basin centre playa lake (Fig. 10b). The SSG–MMG transition therefore represents the southward retreat of the Sherwood-2 River System. The absence of fluvial facies in the upper HSF and TSF in the EISB and Cheshire Basin may be due to preservational bias, as inactive fluvial deposits were rapidly reworked and incorporated into playa margin and aeolian deposits (Lang *et al*. 2004; McKie 2011).

In the EISB and Cheshire Basin, the large volumes of SMF observed (Figs 4 and 6d, e) were deposited in ephemeral lacustrine and dry mudflat settings (Arthurton 1980; Wilson 1990, 1993). The provenance of the MMG has not been directly addressed in this part of the British Isles. Ephemeral lacustrine sediments were probably sourced from distal flash floods, of which the Sherwood-2 River System would have been a contributor. Dry mudflat deposits require fine sediments with an aeolian source. In modern arid settings, fine sediments are highly mobile, and can be transported for hundreds of kilometres by dust storms (Jefferson *et al*. 2002; Brookfield 2008; McKie 2011; Mao *et al*. 2021; Marx *et al*. 2022). Although the nature of lacustrine–aeolian reworking, as well as preservational biases within playa settings, requires further study (McKie 2011), it is probable that not all the mudstone within the SMF has an origin from the Sherwood-2 River System. West-blowing Triassic palaeo-winds may have served to rework sediment into, within and out of these basins (Fig. 10b).

Source areas and regional correlation of the Sherwood-2 River System

Palaeo-lithological domains

Upland areas of pre-Triassic bedrock represent the ultimate source of sediment for the Sherwood-2 River System (Fig. 11). The pre-Triassic surface of northwestern Europe is lithologically diverse, and encompasses an area from the core of the Variscan Orogeny in the south (Baptiste 2016; Martínez Catalán *et al*. 2021) to the Paleozoic sedimentary cover of cratonic Avalonia in the north (Butler 2019).

Although the distribution of basement lithologies during the Triassic is not known, key Variscan basement units had already been exhumed and were supplying sediment to the British Isles by the end of the Carboniferous (*c*. 300 Ma; Hallsworth *et al*. 2000;

Downloaded from https://www.lyellcollection.org by Imperial College of Science, Technology and Medicine on Jul 03, 2026

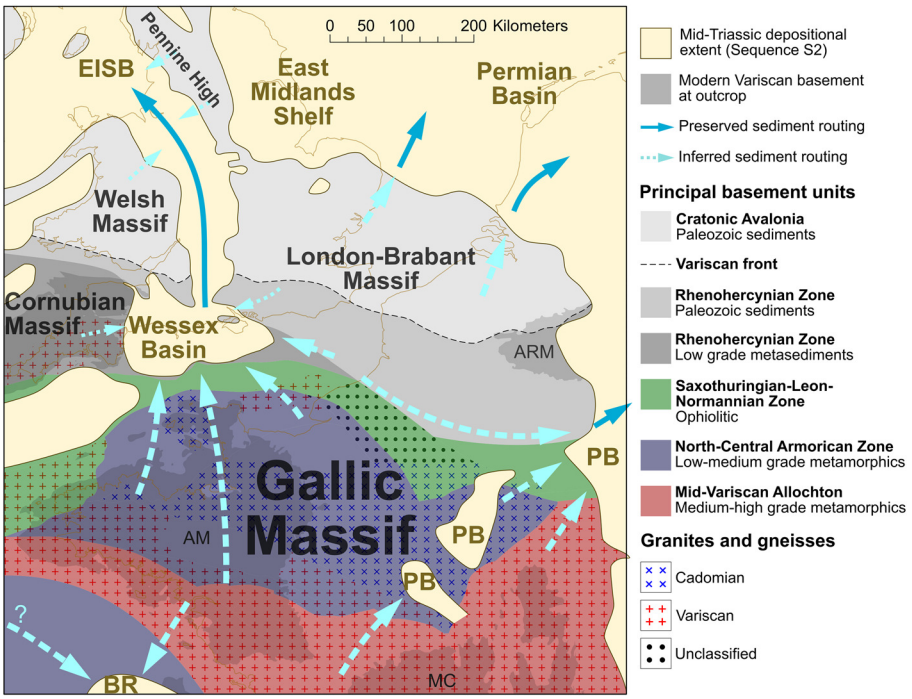


Fig. 11. Triassic sedimentary basins and sediment routing in NW Europe superimposed on a map of first-order Variscan tectonic units. UK basins from Figure 5, and references therein. Basin and sediment routing configuration is portrayed for the mid-Anisian. AM, Armorican Massif; ARM, Ardennes–Rhenish Massif; MC, Massif Central; BR, Biscay Rift; PB, Paris Basin. Source: basins for continental Europe from Bourquin *et al.* (2006), McKie (2017) and Ceccetti *et al.* (2025). Basement lithologies for continental Europe adapted from Mégnien (1980), Baptiste (2016), Laurent *et al.* (2021) and Martínez Catalán *et al.* (2021). Basement lithologies for the English Channel area adapted from Hamblin *et al.* (1992), Shail and Leveridge (2009) and Baptiste (2016). Basement lithologies for the UK adapted from Shail and Leveridge (2009), Butler (2019) and Pullan and Donato (2022).

Jones *et al.* 2011; Morton *et al.* 2021, 2024). The pre-Triassic geology of NW Europe can be categorized by large-scale tectonic domains, each with a differing geological history resulting in a distinct metamorphic, igneous and sedimentary succession. Domains have been characterized using outcropping lithologies, and in places where the pre-Triassic surface is buried under more recent sedimentary cover, using boreholes and geophysical methods (Baptiste 2016; Butler 2019). Where possible, we focus on the distribution of granitoids and gneisses, which provide provenance-sensitive feldspars, zircons and other heavy minerals to their respective fluvial catchments (Paul *et al.* 2008; Sánchez Martínez *et al.* 2012; Tyrrell *et al.* 2012; Morton *et al.* 2013, 2016; Augustsson *et al.* 2018; Sass *et al.* 2023). Additional constraints on sediment routing, including inferences made from known constraints on palaeotopography, can be found in Supplementary material 5.

Internal Variscan metamorphic units

The internal Variscan metamorphic units make up a complex sequence of tectonic domains, which form the core of the Variscan Orogen in NW Europe. The Mid-Variscan Allochthon forms much of the basement in central France (Fig. 11). Variscan-aged granitoids, gneisses and migmatites are found throughout this unit, and are at present the most common group of rocks (Baptiste 2016; Martínez Catalán *et al.* 2021). The North and Central Armorican tectonic domains to the north are primarily composed of metasediments and, respectively, Cadomian-aged granitoids and gneisses and Varican granites (Fig. 11; Baptiste 2016). The northernmost tectonic domain is the Léon–Normannian–Saxothuringian Domain, which lies mostly at subcrop and under the English Channel in the study area, and is poorly characterized (Shail and Leveridge 2009). However, in northern Brittany, this domain contains Variscan granitoids (Martínez Catalán *et al.* 2021). In the east, this domain also contains Cadomian granitoids or gneisses and the Variscan Barfleur Granite (Baptiste 2016; Donato *et al.* 2023).

The Gallic Massif is entirely composed of internal Variscan metamorphic units (Fig. 11). In the Wessex Basin, the delivery of Variscan-aged material to the HSF (Morton *et al.* 2016) necessitates a sediment source in the Central Armorican Zone and Mid-Variscan Allochthon, where the closest Variscan granitoids are concentrated. This yields approximately 300 km of non-preserved drainage for the Sherwood-2 River System over the Gallic Massif (Fig. 11). In the central and eastern Wessex Basin, observed Variscan ages (Morton *et al.* 2016) are probably derived from the Barfleur Granite in northern France, owing to its proximity to the sediment fairway (Fig. 11). In southern Brittany, the Biscay Rift probably directed fluvial systems south towards the Iberian Peninsula (Fig. 11; Péron *et al.* 2005; Bourquin *et al.* 2011; Sánchez Martínez *et al.* 2012). The remaining part of the Gallic Massif is inferred to have supplied the Franco-German Buntsandstein (Fig. 11). This configuration allows for Cadomian and Variscan source signals to be supplied to this latter sediment routing system (Paul *et al.* 2008; Augustsson *et al.* 2018; Sass *et al.* 2023).

Dominantly sedimentary domains

Two basement tectonic domains are predominantly composed of sedimentary rocks: the Rhenohercynian Zone, which represents the Variscan fold-and-thrust belt, and Cratonic Avalonia, which has experienced mild to no Variscan deformation (Fig. 11). Both domains are composed of synorogenic Variscan clastic sediments, as well as carbonates and clastic deposits predating the Variscan Orogeny (e.g. Busby and Smith 2001; Butler 2019; Pharaoh *et al.* 2021). The Rhenohercynian Zone additionally contains Variscan granites of the Cornubian Batholith, with an associated contact metamorphic aureole (Fig. 11; Searle *et al.* 2024). In the Triassic the Rhenohercynian Zone and Cratonic Avalonia would have had a more extensive cover of younger and stratigraphically higher Carboniferous rocks, since removed by erosion.

The catchment for the Sherwood-2 River System probably extended into the Cornubian Batholith in the Rhenohercynian Zone, around 30 km west of the Wessex Basin (Fig. 11) (Smith and Edwards 1991; Morton *et al.* 2013). On the eastern side of the Wessex Basin, the London–Brabant Massif lies in both the Rhenohercynian Zone and Cratonic Avalonia, and has potential to provide a sizeable drainage area into the S2 fairway. However, the extent of the drainage that supplied recycled Devonian clastics from the London–Brabant Massif (Morton *et al.* 2016) is unclear owing

Downloaded from https://www.lyellcollection.org by Imperial College of Science, Technology and Medicine on Jul 03, 2026

to the abundant subcrop of this lithology beneath the Variscan unconformity (Butler 2019). The Welsh Massif also has potential to supply a sizeable drainage area for the S2 fairway (Fig. 10a), and HSF sandstones in the EISB appear to have been derived from North Wales (Mange *et al*. 1999), although the overall extent of this catchment remains unclear. The Pennine High separates the mudstone-dominated East Midlands Shelf from the sandstone-dominated ESIB (Fig. 10a), and was a well-documented sediment source for the latter (Meadows and Beach 1993*a*; Meadows 2006; Scorgie *et al*. 2021; Marsh *et al*. 2022). The Pennine High was probably small in extent and/or elevation, implied by the lack of fluvial activity on the East Midlands Shelf (Howard *et al*. 2009; Jones *et al*. 2025).

Sediment routing over the London–Brabant and Welsh massifs remains poorly known owing to the absence of geological and mineralogical constraints in the Midlands and Worcester Graben. By area, these massifs are the second and third largest uplands after the Gallic Massif (Fig. 11). Regionally, precipitation was highest in the south of the fairway, driven by Tethyan monsoons passing over the Variscan mountains (Péron *et al*. 2005; McKie 2014, 2017). Lastly, the erodibility of the Paleozoic sediments that cover the London–Brabant and Welsh massifs may be several times greater than the metamorphic–granitic basement of the Gallic Massif (Syvitski and Milliman 2007). These lines of evidence suggest that comparatively large sediment fluxes from these uplands may have entered the Sherwood-2 River System in the Worcester Graben or Midlands basins. This sediment was probably lithic-rich and feldspar-poor, containing lithoclasts of metasediments, volcanic rocks, carbonates and chert, and reflecting the mineralogy of recycled Devonian and Carboniferous sandstones (Knox *et al*. 1984; Glover and Powell 1996; Bridge *et al*. 1998; Jones *et al*. 2011). Although bulk sandstone mineralogy clearly changes between the Wessex Basin and the Midlands, lithic fragments of the aforementioned nature are not reported from the northern part of the fairway. Here, lithic fragments are composed of quartz and feldspar by the Gazzi–Dickinson method, which classifies lithic fragments by their constituent mineral phases (Fig. 8b). Hence, changes in bulk mineralogy (Fig. 8b) may not only be a product of interactions between different source areas, but may also result from the breakdown of recycled lithic fragments and feldspar during sediment transport and diagenesis. However, the ability of these processes to alter sandstone mineralogy has been questioned (Frings 2008; Garzanti 2017), and requires quantitative investigation.

Discussion and conclusions

Overall, the stratigraphic architecture of Interval S2 is controlled by an increase in aridity and a series of frequent but brief marine transgressions during the latter part of the Anisian (e.g. McKie 2017; Newell 2017*a*). The Sherwood-2 River System was initially externally draining, but continued aridification meant that for the majority of Interval S2, the fluvial system largely ended in terminal splay systems, discharging into a network of playa lakes with intermittent marine influence. Semiarid fluvial and aeolian deposits of the HSF were gradually replaced by mudstone-dominated playa and halite lake facies of the MMG (Figs 4 and 10a, b).

Within Interval S2, the EISB is the largest sediment sink within the mapped fairway, representing 62% of the total sediment volume deposited during this interval (Fig. 7). Although sand-grade sedimentation ceased during the deposition of the MMG, sediment fluxes were sufficient to fill basins. As previously discussed, calculated sediment accumulation rates were temporally variable and probably controlled by differential tectonic subsidence (Newell 2017*a*), although a paucity of chronostratigraphic constraints within Interval S2 limits the spatio-temporal resolution of this control.

North-flowing palaeocurrents in the HSF (Fig. 10a) and the widespread distribution of Variscan–Cadomian material throughout the sediment fairway (e.g. Mange *et al*. 1999; Plant *et al*. 1999; Tyrrell *et al*. 2012; Morton *et al*. 2016), suggest that the Sherwood-2 River System was one continuous river network. On the other hand, substantial changes in bulk sandstone mineralogy (Fig. 8b) and differences in heavy mineral indices between basins (Plant *et al*. 1999; Morton *et al*. 2013) suggest that sediment composition changes within the fairway. The HSF in the Wessex Basin is dominated by feldspathic sediments supplied from the Gallic Massif, which by area and elevation was the largest catchment feeding the Sherwood-2 River System (Fig. 11). The bulk mineralogy of the HSF in the Wessex Basin contrasts with that of the Midlands basins, Cheshire Basin and EISB, where sediments are substantially more quartz-rich (Fig. 8b). This implies that sediment composition was substantially modified in the Worcester Graben or the Midlands basins (Fig. 8a), probably through substantial tributary input. In the Cheshire Basin and the EISB, fluvial and aeolian inputs of sediment are well documented, and these basins were domains for considerable fluvial–aeolian interactions. Aeolian processes may have continued to be a substantial conveyor of sediment during the deposition of the MMG, and served to both import sediment to and export it from the fairway.

Evidence for additional fluvial inputs into the Sherwood-2 can be further observed when the fluvial systems of the SSG are compared with modern analogues in the Kati Thanda–Lake Eyre Basin (Brookfield 2008; McKie 2014; Morón *et al*. 2014; English *et al*. 2024). Under semiarid climates and with no secondary inputs, these modern river systems experience high water transmission losses of around 80% over approximately 200 km (Costelloe *et al*. 2006), and are mostly ephemeral. Despite a comparable climatic setting, the Sherwood-2 River System was perennial in both its proximal and distal reaches over a length scale of 500 km (Meadows and Beach 1993*a*, *b*; McKie *et al*. 1997; Meadows 2006). As such, secondary fluvial inputs may have been important in maintaining a consistently perennial system, consistent with the substantial sediment inputs into the Sherwood-2 north of the Wessex Basin expressed in bulk sandstone mineralogy. Similarly, the decline of these proximal sources of sand during the onset of aridification may have contributed to generate the SSG–MMG transition. This occurred in the northern part of the fairway despite a sustained semiarid climate in the Wessex Basin (Newell 2017*b*), and a steady supply of fluvial sediment from the Gallic Massif recorded by the time-equivalent HSF (Morton *et al*. 2016).

In conclusion, through the creation of a new chrono- and lithostratigraphic framework, and an updated palaeogeographical framework for the mid-Triassic of the British Isles, we resolve the spatial and temporal dynamics of the HSF, TSF and lower SMF, and construct a source-to-sink depositional model linking the three units. Our new synthesis of bulk sandstone mineralogy, supported by a synthesis of sediment routing and source area lithology, shows that although the Sherwood-2 River System was a single fluvial system, mineralogical changes occur between the south and north parts of the sediment fairway, suggesting that there were probably multiple, substantial sediment inputs north of the Wessex Basin. These tributaries probably drained from the London–Brabant and Welsh massifs into the Midlands basins and Worcester Graben. The temporal evolution of the Sherwood-2 River System was dominated by a southwards retreat of fluvial deposits of the HSF, which were replaced by playa–lacustrine deposition of the TSF and SMF. This change is typically attributed to a regional increase in aridity. However, our results show a greater than fourfold increase in sediment accumulation rate in the EISB, the largest depocentre in the sediment fairway. As such, differential tectonic subsidence was probably a previously unrecognized control on stratigraphic architecture during this time interval.

Downloaded from https://www.lyellcollection.org by Imperial College of Science, Technology and Medicine on Jul 03, 2026

Scientific editing by Rajat Mazumder

Acknowledgements We thank the UK Onshore Geophysical Library, the British Geological Survey, the Bureau de Recherches Géologiques et Minières, EDINA and the North Sea Transition Authority National Data Repository for providing data used for analysis and visualization in this study. We thank N. Meadows and S. Burley for insightful discussions about the Sherwood Sandstone Group, and for supplying petrographic data. We thank P. Burgess and an anonymous reviewer for their comments, which helped improve this paper.

Author contributions **XY**: conceptualization (lead), data curation (lead), formal analysis (lead), investigation (lead), methodology (lead), visualization (lead), writing – original draft (lead), writing – review & editing (equal); **GJH**: funding acquisition (lead), methodology (supporting), supervision (equal), visualization (supporting), writing – review & editing (equal); **ACW**: funding acquisition (supporting), methodology (supporting), supervision (equal), visualization (supporting), writing – review & editing (equal)

Funding This work was funded by the Natural Environment Research Council (Grant NE/S007415/1).

Competing interests The authors declare that they have no known competing financial interests or personal relationships that could have appeared to influence the work reported in this paper.

Data availability All data generated or analysed during this study are included in this published article and its supplementary material files.

References

Ainsworth, N.R. and Riley, L.A. 2010. Triassic to Middle Jurassic stratigraphy of the Kerr McGee 97/12-1 exploration well, offshore southern England. *Marine and Petroleum Geology*, **27**, 853–884, https://doi.org/10.1016/j.marpetgeo.2009.12.014

Ali, A.D. 1982. *Triassic Stratigraphy and Sedimentology in Central England*. Doctoral dissertation, Aston University.

Ali, A.D. and Tuner, P. 1982. Authigenic K-feldspar in the Bromsgrove Sandstone Formation (Triassic) of central England. *Journal of Sedimentary Research*, **52**, 187–197, https://doi.org/10.1306/212F7F09-2B24-11D7-8648000102C1865D

AlNajdi, N. and Worden, R.H. 2023. Porosity in mudstones and its effectiveness for sealing carbon capture and storage sites. *Geological Society, London, Special Publications*, **528**, 339–357, https://doi.org/10.1144/SP528-2022-84

Ambrose, K., Hough, E., Smith, N.J.P. and Warrington, G. 2014. *Lithostratigraphy of the Sherwood Sandstone Group of England, Wales and South-West Scotland*. British Geological Survey Research Report, **RR/14/01**.

Armitage, P.J., Worden, R.H., Faulkner, D.R., Aplin, A.C., Butcher, A.R. and Espie, A.A. 2013. Mercia Mudstone Formation caprock to carbon capture and storage sites: petrology and petrophysical characteristics. *Journal of the Geological Society, London*, **170**, 119–132, https://doi.org/10.1144/jgs2012-049

Arthurton, R.S. 1980. Rhythmic sedimentary sequences in the Triassic Keuper Marl (Mercia Mudstone Group) of Cheshire, northwest England. *Geological Journal*, **15**, 43–58, https://doi.org/10.1002/gj.3350150106

Audley-Charles, M.G. 1970. Triassic palaeogeography of the British Isles. *Quarterly Journal of the Geological Society*, **126**, 49–74, https://doi.org/10.1144/gsjgs.126.1.0049

Augustsson, C. 2021. Influencing factors on petrography interpretations in provenance research – a case-study review. *Geosciences*, **11**, 205, https://doi.org/10.3390/geosciences11050205

Augustsson, C., Voigt, T. *et al.* 2018. Zircon size–age sorting and source-area effect: the German Triassic Buntsandstein Group. *Sedimentary Geology*, **375**, 218–231, https://doi.org/10.1016/j.sedgeo.2017.11.004

Baptiste, J. 2016. *Cartographie Structurale et Lithologique du Substratum du Bassin Parisien et sa Place dans la Chaîne Varisque de l'Europe de l'Ouest: Approches Combinées Géophysiques, Pétrophysiques, Géochronologiques et Modélisations 2D*. Doctoral dissertation, Université d'Orléans.

Barclay, W.J., Ambrose, K., Chadwick, R.A. and Pharaoh, T.C. 1997. *Geology of the Country Around Worcester*. Memoir of the British Geological Survey, Sheet 199 (England and Wales).

Bath, A.H., Milodowski, A.E. and Spiro, B. 1987. Diagenesis of carbonate cements in Permo-Triassic sandstones in the Wessex and East Yorkshire-Lincolnshire Basins, UK: a stable isotope study. *Geological Society, London, Special Publications*, **36**, 173–190, https://doi.org/10.1144/GSL.SP.1987.036.01.14

Benton, M.J. and Spencer, P.S. 1995. British Triassic fossil reptile sites. In: *Fossil Reptiles of Great Britain*. Springer, Dordrecht, https://doi.org/10.1007/978-94-011-0519-4_4

Bourquin, S., Peron, S. and Durand, M. 2006. Lower Triassic sequence stratigraphy of the western part of the Germanic Basin (west of Black Forest): fluvial system evolution through time and space. *Sedimentary Geology*, **186**, 187–211, https://doi.org/10.1016/j.sedgeo.2005.11.018

Bourquin, S., Bercovici, A. *et al.* 2011. The Permian–Triassic transition and the onset of Mesozoic sedimentation at the northwestern peri-Tethyan domain scale: palaeogeographic maps and geodynamic implications. *Palaeogeography, Palaeoclimatology, Palaeoecology*, **299**, 265–280, https://doi.org/10.1016/j.palaeo.2010.11.007

Bowman, M.B.J., McClure, N.M. and Wilkinson, D.W. 1993. Wytch Farm oilfield: deterministic reservoir description of the Triassic Sherwood Sandstone. *Geological Society, London, Petroleum Geology Conference Series*, **4**, 1513–1517, https://doi.org/10.1144/0041513

Bray, R.J., Duddy, I.R. and Green, P.F. 1998. Multiple heating episodes in the Wessex Basin: implications for geological evolution and hydrocarbon generation. *Geological Society, London, Special Publications*, **133**, 199–213, https://doi.org/10.1144/GSL.SP.1998.133.01.09

Bridge, D.McC. and Hough, E. 2002. *Geology of the Wolverhampton and Telford District*. Sheet Description of the British Geological Survey, 1:50 000 Series Sheet 153 (England and Wales).

Bridge, D.McC., Carney, J.N., Lawley, R.S. and Rushton, A.W.A. 1998. *Geology of the Country Around Coventry and Nuneaton*. Memoir of the British Geological Survey, Sheet 169 (England and Wales).

Brookfield, M.E. 2008. Palaeoenvironments and palaeotectonics of the arid to hyperarid intracontinental latest Permian–late Triassic Solway basin (UK). *Sedimentary Geology*, **210**, 27–47, https://doi.org/10.1016/j.sedgeo.2008.06.003

Buchanan, J.G. 1998. The exploration history and controls on hydrocarbon prospectivity in the Wessex basins, southern England, UK. *Geological Society, London, Special Publications*, **133**, 19–37, https://doi.org/10.1144/GSL.SP.1998.133.01.02

Burgess, P.M., Dobromylskyj, E. and Lovell-Kennedy, J. 2025. Probably proximal pebbles? An outcrop-constrained quantitative analysis of clast transport distances in the lower Triassic Sherwood Sandstone Group, UK. *Journal of the Geological Society, London*, **182**, https://doi.org/10.1144/jgs2024-155

Burley, S.D. 1984. Patterns of diagenesis in the Sherwood Sandstone Group (Triassic), United Kingdom. *Clay Minerals*, **19**, 403–440, https://doi.org/10.1180/claymin.1984.019.3.11

Burley, S.D. 1987. *Diagenetic Modelling in the Triassic Sherwood Sandstone Group of England and Its Offshore Equivalents, United Kingdom Continental Shelf*. Doctoral dissertation, University of Hull.

Busby, J.P. and Smith, N.J.P. 2001. The nature of the Variscan basement in southeast England: evidence from integrated potential field modelling. *Geological Magazine*, **138**, 669–685, https://doi.org/10.1017/S0016756801005751

Bushell, T.P. 1986. Reservoir geology of the Morecambe Field. *Geological Society, London, Special Publications*, **23**, 189–208, https://doi.org/10.1144/GSL.SP.1986.023.01.12

Butler, M. 1998. The geological history of the southern Wessex Basin – a review of new information from oil exploration. *Geological Society, London, Special Publications*, **133**, 67–86, https://doi.org/10.1144/GSL.SP.1998.133.01.04

Butler, M. 2019. Seismostratigraphic analysis of Palaeozoic sequences of the Midlands Microcraton. *Geological Society, London, Special Publications*, **471**, 317–332, https://doi.org/10.1144/SP471.6

Carter, A., Yelland, A., Bristow, C. and Hurford, A.J. 1995. Thermal histories of Permian and Triassic basins in Britain derived from fission track analysis. *Geological Society, London, Special Publications*, **91**, 41–56, https://doi.org/10.1144/GSL.SP.1995.091.01.03

Castelltort, S., Fillon, C. *et al.* 2023. *The Source-to-Sink Vade-Mecum: History, Concepts and Tools*, **CSP 16**. Society for Sedimentary Geology, https://doi.org/10.2110/sepmcsp.16

Cecchetti, E., Martinius, A.W., Felder, M., Donselaar, M.E. and Abels, H.A. 2025. Sedimentology, stratigraphy and reservoir architecture of the Lower Triassic Main Buntsandstein in the Roer Valley Graben, the Netherlands. *Marine and Petroleum Geology*, **182**, 107519, https://doi.org/10.1016/j.marpetgeo.2025.107519

Chadwick, R.A. and Evans, D.J. 1995. The timing and direction of Permo-Triassic extension in southern Britain. *Geological Society, London, Special Publications*, **91**, 161–192, https://doi.org/10.1144/GSL.SP.1995.091.01.09

Chadwick, R.A., Jackson, D.I. *et al.* 2001. *Geology of the Isle of Man and its Offshore Area*. British Geological Survey and Treasury Isle of Man, Keyworth, Nottingham.

Charsley, T.J. 1982. *A Standard Nomenclature for the Triassic Formations of the Ashbourne District*. Report of the Institute of Geological Sciences, **81/14**.

Chedburn, L., Underhill, J.R., Head, S. and Jamieson, R. 2022. The critical evaluation of carbon dioxide subsurface storage sites: geological challenges in the depleted fields of Liverpool Bay. *AAPG Bulletin*, **106**, 1753–1789, https://doi.org/10.1306/07062221120

Chisholm, J.I., Charsley, T.J. and Aitkenhead, N. 1988. *Geology of the Country Around Ashbourne and Cheadle*. Memoir of the British Geological Survey, Sheet 124.

Coram, R.A., Radley, J.D. and Benton, M.J.. 2019 The Middle Triassic (Anisian) Otter Sandstone biota (Devon, UK): review, recent discoveries and ways ahead. *Proceedings of the Geologists' Association*, **130**, 294–306, https://doi.org/10.1016/j.pgeola.2017.06.007

Downloaded from https://www.lyellcollection.org by Imperial College of Science, Technology and Medicine on Jul 03, 2026

Cosgrove, G.I., Alkathery, M., Al-Masrahy, M., Colombera, L., Mountney, N.P. and Thompson, D.B. 2025. Quantitative sedimentological analysis of the aeolian–fluvial Triassic Sherwood Sandstone Group, Cheshire Basin, UK. *Sedimentology*, **72**, 1233–1274, https://doi.org/10.1111/sed.70000

Costelloe, J.F., Grayson, R.B. and McMahon, T.A. 2006. Modelling streamflow in a large anastomosing river of the arid zone, Diamantina River, Australia. *Journal of Hydrology*, **323**, 138–153, https://doi.org/10.1016/j.jhydrol.2005.08.022

Cowan, G. 1993. Identification and significance of aeolian deposits within the dominantly fluvial Sherwood Sandstone Group of the East Irish Sea Basin UK. *Geological Society, London, Special Publications*, **73**, 231–245, https://doi.org/10.1144/GSL.SP.1993.073.01.14

Croker, P. and Shannon, P. 1987. The evolution and hydrocarbon prospectivity of the Porcupine Basin, offshore Ireland. Conference on Petroleum Geology of North West Europe, 26–29 October, **3**, London, 633–642.

Dercourt, J., Gaetani, M. *et al.* 2000. *Atlas Peri-Tethys – Palaeogeographical Maps*. CCGM/CGMW, Paris.

De Sainz Simpson, R. 2022. *Sherwood Sandstone Outcrop Analogues Study in the Cheshire Basin: How to Better Constrain CCS Potential and CO_2 Injectability in Depleted Oil and Gas Fields in the Context of the Liverpool Bay Carbon Capture Project*. Master's thesis, University of Manchester.

DiGRock250k 2013. [SHAPE geospatial data], Scale 1:250000, Tiles: GB, updated 31 December 2013, BGS, using EDINA Geology Digimap Service, https://digimap.edina.ac.uk [downloaded 17 July 2024].

DiGRock625k 2008. [SHAPE geospatial data], Scale 1:625000, Tiles: GB, updated 31 December 2008, BGS, using Ordinance Survey, https://osdatahub.os.uk/ [downloaded 23 November 2023].

Donato, J.A., Pullan, C.P. and Dimitropoulos, K. 2023. *Moho Topography Beneath England, The Regional Gravity Field and Speculations on Crustal Structure*. UK Onshore Geophysical Library.

Downing, R.A., Allen, D.J., Barker, J.A., Burgess, W.G., Gray, D.A., Price, M. and Smith, I.F. 1984. Geothermal exploration at Southampton in the UK: a case study of a low enthalpy resource. *Energy Exploration and Exploitation*, **2**, 327–342, https://doi.org/10.1177/014459878400200404

Dunford, G.M., Dancer, P.N. and Long, K.D. 2001. Hydrocarbon potential of the Kish Bank Basin: integration within a regional model for the Greater Irish Sea Basin. *Geological Society, London, Special Publications*, **188**, 135–154, https://doi.org/10.1144/GSL.SP.2001.188.01.07

Earp, J.R. and Taylor, B.J. 1986. *Geology of the Country Around Chester and Winsford*. Memoir of the British Geological Survey, Sheet 109 (England and Wales).

Edwards, R.A. 1999. *The Minehead District: A Concise Account of the Geology*. Memoir of the British Geological Survey, Sheet 278 and Part of Sheet 294 (England and Wales). Stationery Office.

English, K.L., English, J.M., Moscardini, R., Haughton, P.D., Raine, R.J. and Cooper, M. 2024. Review of Triassic Sherwood Sandstone Group reservoirs of Ireland and Great Britain and their future role in geoenergy applications. *Geoenergy*, **2**, https://doi.org/10.1144/geoenergy2023-042

Evans, D.J. and Holloway, S. 2009. A review of onshore UK salt deposits and their potential for underground gas storage. *Geological Society, London, Special Publications*, **313**, 39–80, https://doi.org/10.1144/SP313.5

Evans, D.J., Rees, J.G. and Holloway, S. 1993. The Permian to Jurassic stratigraphy and structural evolution of the central Cheshire Basin. *Journal of the Geological Society, London*, **150**, 857–870, https://doi.org/10.1144/gsjgs.150.5.0857

Evans, D.J., Williams, J.D.O., Hough, E. and Stacey, A. 2011. The stratigraphy and lateral correlations of the Northwich and Preesall halites from the Cheshire Basin–East Irish Sea areas: implications for sedimentary environments, rates of deposition and the solution mining of gas storage caverns. *In*: SMRI Fall 2011 Technical Conference, 2–4 October 2011, York.

Floodpage, J., Newman, P. and White, J. 2001. Hydrocarbon prospectivity in the Irish Sea area: insights from recent exploration of the Central Irish Sea, Peel and Solway basins. *Geological Society, London, Special Publications*, **188**, 107–134, https://doi.org/10.1144/GSL.SP.2001.188.01.06

Franklin, J., Tyrrell, S., O'Sullivan, G., Nauton-Fourteu, M. and Raine, R. 2020. Provenance of Triassic sandstones in the basins of Northern Ireland – implications for NW European Triassic palaeodrainage. *Geological Journal*, **55**, 5432–5450, https://doi.org/10.1002/gj.3697

Frings, R.M. 2008. Downstream fining in large sand-bed rivers. *Earth-Science Reviews*, **87**, 39–60, https://doi.org/10.1016/j.earscirev.2007.10.001

Garzanti, E. 2017. The maturity myth in sedimentology and provenance analysis. *Journal of Sedimentary Research*, **87**, 353–365, https://doi.org/10.2110/jsr.2017.17

Garzanti, E. 2019. Petrographic classification of sand and sandstone. *Earth-Science Reviews*, **192**, 545–563, https://doi.org/10.1016/j.earscirev.2018.12.014

Gent, C.M.A. 2016. *Maturity Modelling of Well 110/07b-6*. British Geological Survey Commissioned Report, **CR/16/043**.

Gibson-Poole, C.M., Tarasewicz, J. *et al.* 2026. Endurance saline aquifer CO_2 store – from appraisal to development and beyond. *Geological Society, London, Energy Geoscience Conference Series*, **1**, https://doi.org/10.1144/egc1-2024-23

Glover, B.W. and Powell, J.H. 1996. Interaction of climate and tectonics upon alluvial architecture: late Carboniferous–Early Permian sequences at the southern margin of the Pennine Basin, UK. *Palaeogeography, Palaeoclimatology, Palaeoecology*, **121**, 13–34, https://doi.org/10.1016/0031-0182(95)00050-X

Green, P.F., Thomson, K. and Hudson, J.D. 2001. Recognition of tectonic events in undeformed regions: contrasting results from the Midland Platform and East Midlands Shelf, Central England. *Journal of the Geological Society, London*, **158**, 59–73, https://doi.org/10.1144/jgs.158.1.59

Greenwood, P.J. and Habesch, S.M. 1997. Diagenesis of the Sherwood Sandstone Group in the southern East Irish Sea Basin (Blocks 110/13, 110/14 and 110/15): constraints from preliminary isotopic and fluid inclusion studies. *Geological Society, London, Special Publications*, **124**, 353–371, https://doi.org/10.1144/GSL.SP.1997.124.01.21

Hallsworth, C.R., Morton, A.C., Claoué-Long, J. and Fanning, C.M. 2000. Carboniferous sand provenance in the Pennine Basin, UK: constraints from heavy mineral and detrital zircon age data. *Sedimentary Geology*, **137**, 147–185, https://doi.org/10.1016/S0037-0738(00)00153-6

Hamblin, R.J.O., Crosby, A., Balson, P.S., Jones, S.M., Chadwick, R.A., Penn, I.E. and Arthur, M.J. 1992. *United Kingdom Offshore Regional Report. The Geology of the English Channel*. HMSO for the British Geological Survey, London.

Hampson, G.J., Duller, R.A., Petter, A.L., Robinson, R.A.J. and Allen, P.A. 2014. Mass-balance constraints on stratigraphic interpretation of linked alluvial–coastal-shelf deposits from source to sink: example from Cretaceous Western Interior Basin, Utah and Colorado, U.S.A. *Journal of Sedimentary Research*, **84**, 935–960, https://doi.org/10.2110/jsr.2014.78

Hawkes, P.W., Fraser, A.J. and Einchcomb, C.C.G. 1998. The tectono-stratigraphic development and exploration history of the Weald and Wessex basins, Southern England, UK. *Geological Society, London, Special Publications*, **133**, 39–65, https://doi.org/10.1144/GSL.SP.1998.133.01.03

Head, S., Underhill, J.R., Jamieson, R. and Busch, A. 2026. Evaluating the role of cap rock in controlling natural accumulation and storage of carbon dioxide in the East Irish Sea Basin, UK. *Geological Society, London, Energy Geoscience Conference Series*, **1**, https://doi.org/10.1144/egc1-2024-10

Helland-Hansen, W., Sømme, T.O., Martinsen, O.J., Lunt, I. and Thurmond, J. 2016. Deciphering Earth's natural hourglasses; perspectives on source-to-sink analysis. *Journal of Sedimentary Research*, **86**, 1008–1033, https://doi.org/10.2110/jsr.2016.56

Herries, R.D. and Cowan, G. 1997. Challenging the 'sheetflood' myth: the role of water-table-controlled sabkha deposits in redefining the depositional model for the Ormskirk Sandstone Formation (Lower Triassic), East Irish Sea Basin. *Geological Society, London, Special Publications*, **124**, 253–276, https://doi.org/10.1144/GSL.SP.1997.124.01.16

Holliday, D.W., Williams, G.M., Holloway, S., Savage, D. and Bannon, M.P. 1991. *A Preliminary Feasibility Study for the Underground Disposal of Carbon Dioxide in UK*. British Geological Survey, Nottingham (**WE/91/020**) [unpublished].

Hough, E. 2002. Geology of the north Wirral district. British Geological Survey Internal Report, WA/98/66.

Hounslow, M.W. and Gallois, R. 2023. Magnetostratigraphy of the Mercia Mudstone Group (Devon, UK): implications for regional relationships and chronostratigraphy in the Middle to Late Triassic of Western Europe. *Journal of the Geological Society, London*, **180**, https://doi.org/10.1144/jgs2022-173

Hounslow, M.W. and McIntosh, G. 2003. Magnetostratigraphy of the Sherwood Sandstone Group (Lower and Middle Triassic), south Devon, UK: detailed correlation of the marine and non-marine Anisian. *Palaeogeography, Palaeoclimatology, Palaeoecology*, **193**, 325–348, https://doi.org/10.1016/S0031-0182(03)00235-9

Hounslow, M.W., McIntosh, G., Edwards, R.A., Laming, D.J. and Karloukovski, V. 2017. End of the Kiaman Superchron in the Permian of SW England: magnetostratigraphy of the Aylesbeare Mudstone and Exeter groups. *Journal of the Geological Society, London*, **174**, 56–74, https://doi.org/10.1144/jgs2015-141

Howard, A.S., Warrington, G., Ambrose, K. and Rees, J.G. 2008. *A Formational Framework for the Mercia Mudstone Group (Triassic) of England and Wales*. British Geological Survey Research Report, **RR/08/04**.

Howard, A., Warrington, G., Carney, J., Ambrose, K., Young, S.R., Pharaoh, T. and Cheney, C. 2009. *Geology of the Nottingham District: Memoir for 1:50 000 Geological Sheet 126 (England and Wales)*. British Geological Survey.

Jackson, D.I., Jackson, A.A., Evans, D., Wingfield, R.T.R., Barnes, R.P. and Arthur, M.J. 1995. *United Kingdom Offshore Regional Report: The Geology of the Irish Sea*. HMSO for the British Geological Survey, London.

Jackson, D.I., Johnson, H. and Smith, N.J.P. 1997. Stratigraphical relationships and a revised lithostratigraphical nomenclature for the Carboniferous, Permian and Triassic rocks of the offshore East Irish Sea Basin. *Geological Society, London, Special Publications*, **124**, 11–32, https://doi.org/10.1144/GSL.SP.1997.124.01.02

Jeans, C.V. 2006. Clay mineralogy of the Permo-Triassic strata of the British Isles: onshore and offshore. *Clay Minerals*, **41**, 309–354, https://doi.org/10.1180/0009855064110199

Jefferson, I., Rosenbaum, M. and Smalley, I. 2002. Mercia Mudstone as a Triassic aeolian desert sediment. *Mercian Geologist*, **15**, 157–162.

Jones, N.S. and Ambrose, K. 1994. Triassic sandy braidplain and aeolian sedimentation in the Sherwood Sandstone Group of the Sellafield area, west Cumbria. *Proceedings of the Yorkshire Geological Society*, **50**, 61–76, https://doi.org/10.1144/pygs.50.1.61

Jones, N.S., Holliday, D.W. and McKervey, J.A. 2011. Warwickshire Group (Pennsylvanian) red-beds of the Canonbie Coalfield, England–Scotland

Downloaded from https://www.lyellcollection.org by Imperial College of Science, Technology and Medicine on Jul 03, 2026

border, and their regional palaeogeographical implications. *Geological Magazine*, **148**, 50–77, https://doi.org/10.1017/S001675681000035X

Jones, S.T., Worden, R.H., Faulkner, D.R., Fisher, Q.J., McEvoy, J.A. and Utley, J.E. 2025. Deposition, diagenesis, and porosity of a siliciclastic caprock: the Late Triassic Mercia Mudstone Group. *Journal of the Geological Society, London*, **182**, https://doi.org/10.1144/jgs2025-086

Knox, R.O.B., Burgess, W.G., Wilson, K.S. and Bath, A.H. 1984. Diagenetic influences on reservoir properties of the Sherwood Sandstone (Triassic) in the Marchwood geothermal borehole, Southampton, UK. *Clay Minerals*, **19**, 441–456, https://doi.org/10.1180/claymin.1984.019.3.12

Lang, S.C., Payenberg, T.H.D., Reilly, M.R.W., Hicks, T., Benson, J. and Kassan, J. 2004. Modern analogues for dryland sandy fluvial–lacustrine deltas and terminal splay reservoirs. *APPEA Journal*, **44**, 329–356, https://doi.org/10.1071/AJ03012

Laurent, A., Averbuch, O., Beccaletto, L., Graveleau, F., Lacquement, F., Capar, L. and Marc, S. 2021. 3-D structure of the Variscan thrust front in northern France: new insights from seismic reflection profiles. *Tectonics*, **40**, p.e2020TC006642, https://doi.org/10.1029/2020TC006642

Mange, M., Turner, P., Ince, D., Pugh, J. and Wright, D. 1999. A new perspective on the zonation and correlation of barren strata: an integrated heavy mineral and palaeomagnetic study of the Sherwood Sandstone Group, East Irish Sea Basin and surrounding areas. *Journal of Petroleum Geology*, **22**, 325–348, https://doi.org/10.1111/j.1747-5457.1999.tb00990.x

Mange, M.A., Turner, P., Ince, D. and Wright, D.T. 2007. High-resolution heavy mineral- and magnetostratigraphy; a powerful tool for subdivision and correlation of barren successions: an example from the Sherwood Sandstone Group (Triassic) of the East Irish Sea Basin and surrounding areas. *Developments in Sedimentology*, **58**, 1073–1097, https://doi.org/10.1016/S0070-4571(07)58042-8

Mao, X., Liu, X. and Zhou, X. 2021. Permo-Triassic aeolian red clay of southwestern England and its palaeoenvironmental implications. *Aeolian Research*, **52**, https://doi.org/10.1016/j.aeolia.2021.100726

Markwick, P.J. 2019. Palaeogeography in exploration. *Geological Magazine*, **156**, 366–407, https://doi.org/10.1017/S0016756818000468

Marsh, J.R., Jones, S.J., Meadows, N.S. and Gluyas, J.G. 2022. Petrographic and diagenetic investigation of the distal Triassic 'Budleighensis' fluvial system in the Solway and Carlisle Basins for potential CO_2 storage. *Petroleum Geoscience*, **28**, https://doi.org/10.1144/petgeo2021-065

Martínez Catalán, J.R., Schulmann, K. and Ghienne, J.F. 2021. The Mid-Variscan Allochthon: keys from correlation, partial retrodeformation and plate-tectonic reconstruction to unlock the geometry of a non-cylindrical belt. *Earth-Science Reviews*, **220**, https://doi.org/10.1016/j.earscirev.2021.103700

Marx, S.K., May, J.-H., Cohen, T., Kamber, B.S., McGowan, H.A. and Petherick, L. 2022. Dust emissions from Kati Thanda–Lake Eyre: a review. *Transactions of the Royal Society of South Australia*, **146**, 168–206, https://doi.org/10.1080/03721426.2022.2054918

McKie, T. 2011. A comparison of modern Dryland depositional systems with the Rotliegend group in the Netherlands. *SEPM Special Publications*, **98**, 89–103, https://doi.org/10.2110/pec.11.98.0089

McKie, T. 2014. Climatic and tectonic controls on Triassic dryland terminal fluvial system architecture, central North Sea. *IAS Special Publication*, **46**, 19–58, https://doi.org/10.1002/9781118920435.ch2

McKie, T. 2017. Palaeogeographic evolution of latest Permian and Triassic salt basins in Northwest Europe. *In*: Soto, J.I., Flinch, J.F. and Tari, G. (eds) *Permo-Triassic Salt Provinces of Europe, North Africa and the Atlantic Margins*. Elsevier, 159–173, https://doi.org/10.1016/B978-0-12-809417-4.00008-2

McKie, T., Aggett, J. and Hogg, A.J.C. 1997. Sequence architecture of a Triassic semi-arid, fluvio-lacustrine reservoir, Wytch Farm Field, southern England. *In*: GCSSEPM Foundation 18th Annual Research Conference Shallow Marine and Nonmarine Reservoirs, Austin, TX, 7–10 December 1997, https://doi.org/10.5724/gcs.97.18.0197

Meadows, N.S. 2004. *Modals 110-12a-1, 110-12a-6, 110-13-10, Pet EISB + Cheshire* [unpublished data].

Meadows, N.S. 2006. The correlation and sequence architecture of the Ormskirk Sandstone Formation in the Triassic Sherwood Sandstone Group of the East Irish Sea Basin, NW England. *Geological Journal*, **41**, 93–122, https://doi.org/10.1002/gj.1034

Meadows, N.S. and Beach, A. 1993*a*. Controls on reservoir quality in the Triassic Sherwood Sandstone of the Irish Sea. *Geological Society, London, Petroleum Geology Conference Series*, **4**, 823–833, https://doi.org/10.1144/0040823

Meadows, N.S. and Beach, A. 1993*b*. Structural and climatic controls on facies distribution in a mixed fluvial and aeolian reservoir: the Triassic Sherwood Sandstone in the Irish Sea. *Geological Society, London, Special Publications*, **73**, 247–264, https://doi.org/10.1144/GSL.SP.1993.073.01.15

Medici, G., West, L.J. and Mountney, N.P. 2019*a*. Sedimentary flow heterogeneities in the Triassic UK Sherwood Sandstone Group: insights for hydrocarbon exploration. *Geological Journal*, **54**, 1361–1378, https://doi.org/10.1002/gj.3233

Medici, G., West, L.J., Mountney, N.P. and Welch, M. 2019*b*. Permeability of rock discontinuities and faults in the Triassic Sherwood Sandstone Group (UK): insights for management of fluvio-aeolian aquifers worldwide. *Hydrogeology Journal*, **27**, 2835–2855, https://doi.org/10.1007/s10040-019-02035-7

Mégnien, C. 1980. *Synthèse géologique du bassin de Paris*. Editions du BRGM, vol. 2. Mémoires du BRGM, no. 103.

Merlin Energy Resources Consortium 2020. *The Standard Stratigraphic Nomenclature of Offshore Ireland: An Integrated Lithostratigraphic, Biostratigraphic and Sequence Stratigraphic Framework. Project Atlas*. Petroleum Affairs Division, Department of the Environment (DEEC), Climate and Communications, Special Publication, **1/21**.

Michael, N.A. and Zühlke, R. 2022. Source-to-sink: regional grain size trends to reconstruct sediment budgets and catchment areas. *Basin Research*, **34**, 393–410, https://doi.org/10.1111/bre.12624

Mikkelsen, P.W. and Floodpage, J.B. 1997. The hydrocarbon potential of the Cheshire Basin. *Geological Society, London, Special Publications*, **124**, 161–183, https://doi.org/10.1144/GSL.SP.1997.124.01.10

Miliorizos, M. and Ruffell, A. 1998. Kinematics of the Watchet–Cothelstone–Hatch fault system: implications for the fault history of the Wessex basin and adjacent areas. *Geological Society, London, Special Publications*, **133**, 311–330, https://doi.org/10.1144/GSL.SP.1998.133.01.15

Morón, S., Amos, K. and Mann, S. 2014. Fluvial reservoirs in dryland endorheic basins: the Lake Eyre Basin as a world-class modern analogue. *APPEA Journal*, **54**, 119–134, https://doi.org/10.1071/AJ13014

Morton, A.C. and Hallsworth, C. 1994. Identifying provenance-specific features of detrital heavy mineral assemblages in sandstones. *Sedimentary Geology*, **90**, 241–256, https://doi.org/10.1016/0037-0738(94)90041-8

Morton, A., Hounslow, M.W. and Frei, D. 2013. Heavy-mineral, mineral-chemical and zircon-age constraints on the provenance of Triassic sandstones from the Devon coast, southern Britain. *Geologos*, **19**, 67–85, https://doi.org/10.2478/logos-2013-0005

Morton, A., Knox, R. and Frei, D. 2016. Heavy mineral and zircon age constraints on provenance of the Sherwood Sandstone Group (Triassic) in the eastern Wessex Basin, UK. *Proceedings of the Geologists' Association*, **127**, 514–526, https://doi.org/10.1016/j.pgeola.2016.06.001

Morton, A.C., Chisholm, J.I. and Frei, D. 2021. Provenance of Carboniferous sandstones in the central and southern parts of the Pennine Basin, UK: evidence from detrital zircon ages. *Proceedings of the Yorkshire Geological Society*, **63**, https://doi.org/10.1144/pygs2020-010

Morton, A.C., Chisholm, J.I. and Frei, D. 2024. Provenance response to evolving palaeogeography recorded by Carboniferous sandstones in the northern Pennine Basin, UK. *Sedimentary Geology*, **470**, https://doi.org/10.1016/j.sedgeo.2024.106691

Moscardini, R.I., English, K.L., Raine, R., Haughton, P.D., English, J.M. and Cooper, M. 2025. Reservoir heterogeneity in the Triassic Sherwood Sandstone Group: new insights from the Larne Basin, Northern Ireland. *Geoenergy*, **3**, geoenergy2025-015, https://doi.org/10.1144/geoenergy2025-015

Mountney, N.P. and Thompson, D.B. 2002. Stratigraphic evolution and preservation of aeolian dune and damp/wet interdune strata: an example from the Triassic Helsby Sandstone Formation, Cheshire Basin, UK. *Sedimentology*, **49**, 805–833, https://doi.org/10.1046/j.1365-3091.2002.00472.x

Naylor, D., Haughey, N., Clayton, G. and Graham, J.R. 1993. The Kish Bank Basin, offshore Ireland. *Geological Society, London, Petroleum Geology Conference Series*, **4**, 845–855, https://doi.org/10.1144/0040845

Newell, A.J. 2017*a*. Rifts, rivers and climate recovery: a new model for the Triassic of England. *Proceedings of the Geologists' Association*, **129**, 352–371, https://doi.org/10.1016/j.pgeola.2017.04.001

Newell, A.J. 2017*b*. Evolving stratigraphy of a Middle Triassic fluvial-dominated sheet sandstone: the Otter Sandstone Formation of the Wessex Basin (UK). *Geological Journal*, **53**, 1954–1972, https://doi.org/10.1002/gj.3026

Newell, A.J. 2023. *The Sherwood Sandstone and Bacton Groups of the East Midlands Shelf – An Onshore to Offshore Correlation Using Outcrop Evidence and Geophysical Logs*. British Geological Survey, Nottingham.

Newell, A. 2024. *UK Stratigraphical Framework Series: Mercia Mudstone Group*. British Geological Survey Open Report, **OR/24/046**.

Newell, A.J. and Shariatipour, S.M. 2016. Linking outcrop analogue with flow simulation to reduce uncertainty in sub-surface carbon capture and storage: an example from the Sherwood Sandstone Group of the Wessex Basin, UK. *Geological Society, London, Special Publications*, **436**, 231–246, https://doi.org/10.1144/SP436.2

Newell, A.J. and Smith, N.J. 2009. *Bromsgrove Aquifer Groundwater Modelling Study: Results from Task 1.1 3D Visualisation and Geological Framework of the Bromsgrove Aquifer*. British Geological Survey Commissioned Report, **CR/09/023**.

Newman, P.J. 1999. The geology and hydrocarbon potential of the Peel and Solway Basins, East Irish Sea. *Journal of Petroleum Geology*, **22**, 305–324, https://doi.org/10.1111/j.1747-5457.1999.tb00989.x

Ogg, J.G., Chen, Z.-Q., Orchard, M.J. and Jiang, H.S. 2020. The Triassic Period. *In*: Gradstein, F.M., Ogg, J.G., Schmitz, M.D. and Ogg, G.M. (eds) *Geologic Time Scale*. Elsevier, 903–953, https://doi.org/10.1016/B978-0-12-824360-2.00025-5

Old, R.A., Sumbler, M.G. and Ambrose, K. 1987. *Geology of the Country Around Warwick*. Memoir of the British Geological Survey, Sheet 184 (England and Wales).

Old, R.A., Hamblin, R.J.O., Ambrose, K. and Warrington, G. 1991. *Geology of the Country Around Redditch*. Memoir of the British Geological Survey, Sheet 183 (England and Wales).

Paola, C. and Martin, J.M. 2012. Mass-balance effects in depositional systems. *Journal of Sedimentary Research*, **82**, 435–450, https://doi.org/10.2110/jsr.2012.38

Downloaded from https://www.lyellcollection.org by Imperial College of Science, Technology and Medicine on Jul 03, 2026

Parkes, D., Busby, J., Kemp, S.J., Petitclerc, E. and Mounteney, I. 2021. The thermal properties of the Mercia Mudstone Group. *Quarterly Journal of Engineering Geology and Hydrogeology*, **54**, https://doi.org/10.1144/qjegh2020-098

Paul, J., Wemmer, K. and Ahrendt, H. 2008. Provenance of siliciclastic sediments (Permian to Jurassic) in the Central European Basin. *Zeitschrift der Deutschen Gesellschaft für Geowissenschaften*, **159**, 641–650, https://doi.org/10.1127/1860-1804/2008/0159-0641

Péron, S., Bourquin, S., Fluteau, F. and Guillocheau, F. 2005. Palaeoenvironment reconstructions and climate simulations of the Early Triassic: impact of the water and sediment supply on the preservation of fluvial systems. *Geodinamica Acta*, **18**, 431–446, https://doi.org/10.3166/ga.18.431-446

Pharaoh, T.C., Gent, C.M.A. *et al.* 2019. An overlooked play? Structure, stratigraphy and hydrocarbon prospectivity of the Carboniferous in the East Irish Sea–North Channel basin complex. *Geological Society, London, Special Publications*, **471**, 281–316, https://doi.org/10.1144/SP471.7

Pharaoh, T., Jones, D. *et al.* 2021. Early Carboniferous limestones of southern and central Britain: characterisation and preliminary assessment of deep geothermal prospectivity. *Zeitschrift der Deutschen Gesellschaft für Geowissenschaften*, **172**, 227–249, https://doi.org/10.1127/zdgg/2021/0282

Plant, J.A., Jones, D.G. and Haslam, H.W. (eds) 1999. *The Cheshire Basin: Basin Evolution, Fluid Movement and Mineral Resources in a Permo-Triassic Rift Setting*. For the British Geological Survey, Keyworth, Nottingham.

Pullan, C.P. and Donato, J.A. 2022. *The Eastern Extension of Southwest England Under the Mesozoic Southern England Basin and its Variscan Dextral Translation*. UK Onshore Geophysical Library.

Radley, J.D. and Coram, R.A. 2016. The Chester Formation (Early Triassic, southern Britain): sedimentary response to extreme greenhouse climate? *Proceedings of the Geologists' Association*, **127**, 552–557, https://doi.org/10.1016/j.pgeola.2016.08.002

Ravidà, D.C., Caracciolo, L., Heins, W.A. and Stollhofen, H. 2021. Reconstructing environmental signals across the Permian–Triassic boundary in the SE Germanic basin: palaeodrainage modelling and quantification of sediment flux. *Global and Planetary Change*, **206**.

Rees, J.G. and Wilson, A.A. 1998. *Geology of the Country Around Stoke-on-Trent*. Memoir of the Geological Survey, Sheet 123 (England and Wales).

Reynolds, T. 2024. Grain size from source to sink – modern and ancient fining rates. *Earth-Science Reviews*, **250**, https://doi.org/10.1016/j.earscirev.2024.104699

Rhys, G.H. 1982. *The Winterborne Kingston Borehole, Dorset, England*. Report of the Institute of Geological Sciences, **81/3**.

Romans, B.W. and Graham, S.A. 2013. A deep-time perspective of land–ocean linkages in the sedimentary record. *Annual Review of Marine Science*, **5**, 69–94, https://doi.org/10.1146/annurev-marine-121211-172426

Sánchez Martínez, S., De la Horra, R. *et al.* 2012. U–Pb ages of detrital zircons from the Permo-Triassic series of the Iberian Ranges: a record of variable provenance during rift propagation. *Journal of Geology*, **120**, 135–154, https://doi.org/10.1086/663983

Sass, K., von Eynatten, H., Meyerink, T., Schade, J. and Dunkl, I. 2023. Heavy mineral constraints on the evolution and provenance of upper Permian and lower Triassic siliciclastic deposits of the Central European Basin. *Zeitschrift der Deutschen Gesellschaft für Geowissenschaften*, **174**, https://doi.org/10.1127/zdgg/2023/0404

Scorgie, J.C., Worden, R.H., Utley, J.E.P. and Roche, I.P. 2021. Reservoir quality and diagenesis of Triassic sandstones and siltstones from arid fluvial and playa margin environments: a study of one of the UK's earliest producing oilfields. *Marine and Petroleum Geology*, **131**, https://doi.org/10.1016/j.marpetgeo.2021.105154

Searle, M.P., Shail, R.K., Pownall, J.M., Jurkowski, C., Watts, A.B. and Robb, L.J. 2024. The Permian Cornubian granite batholith, SW England; part 1: field, structural, and petrological constraints. *Geological Society of America Bulletin*, **136**, 4301–4320, https://doi.org/10.1130/B37457.1

Shail, R.K. and Leveridge, B.E. 2009. The Rhenohercynian passive margin of SW England: development, inversion and extensional reactivation. *Comptes Rendus, Géoscience*, **341**, 140–155, https://doi.org/10.1016/j.crte.2008.11.002

Simms, M. 2009. The Permian and Mesozoic. *In*: Holland, C.H. and Sanders, I. (eds) *The Geology of Ireland*. Liverpool University Press, 331–332, https://doi.org/10.2307/jj.12638997.16

Smith, S.A. and Edwards, R.A. 1991. Regional sedimentological variations in Lower Triassic fluvial conglomerates (Budleigh Salterton Pebble Beds), southwest England: some implications for palaeogeography and basin evolution. *Geological Journal*, **26**, 65–83, https://doi.org/10.1002/gj.3350260105

Sømme, T.O., Helland-Hansen, W., Martinsen, O.J. and Thurmond, J.B. 2009. Relationships between morphological and sedimentological parameters in source-to-sink systems: a basis for predicting semi-quantitative characteristics in subsurface systems. *Basin Research*, **21**, 361–387, https://doi.org/10.1111/j.1365-2117.2009.00397.x

Strong, G.E. and Milodowski, A.E. 1987. Aspects of the diagenesis of the Sherwood Sandstones of the Wessex Basin and their influence on reservoir characteristics. *Geological Society, London, Special Publications*, **36**, 325–337, https://doi.org/10.1144/GSL.SP.1987.036.01.23

Sumbler, M.G., Barron, A.J.M. and Morigi, A.N. 2000. *Geology of the Cirencester District*. Memoir of the British Geological Survey, Sheet 235 (England and Wales).

Sun, Y., Joachimski, M.M. *et al.* 2012. Lethally hot temperatures during the Early Triassic greenhouse. *Science*, **338**, 366–370, https://doi.org/10.1126/science.1224126

Svendsen, J.B. and Hartley, N.R. 2001. Comparison between outcrop-spectral gamma ray logging and whole rock geochemistry: implications for quantitative reservoir characterisation in continental sequences. *Marine and Petroleum Geology*, **18**, 657–670, https://doi.org/10.1016/S0264-8172(01)00022-8

Syvitski, J.P. and Milliman, J.D. 2007. Geology, geography, and humans battle for dominance over the delivery of fluvial sediment to the coastal ocean. *Journal of Geology*, **115**, 1–19, https://doi.org/10.1086/509246

Thomas, L.P. and Holliday, D.W. 1982. *Southampton No. 1 (Western Esplanade) Geothermal Well: Geological Well Completion Report*, **WA/KB/82/003**. Institute of Geological Sciences [unpublished].

Thompson, D.B. 1970*a*. The stratigraphy of the so-called Keuper Sandstone Formation (Scythian–? Anisian) in the Permo–Triassic Cheshire Basin. *Quarterly Journal of the Geological Society*, **126**, 151–181, https://doi.org/10.1144/gsjgs.126.1.0151

Thompson, D.B. 1970*b*. Sedimentation of the Triassic (Scythian) red pebbly sandstones in the Cheshire Basin and its margins. *Geological Journal*, **7**, 183–216, https://doi.org/10.1002/gj.3350070111

Thompson, J. and Meadows, N.S. 1997. Clastic sabkhas and diachroneity at the top of the Sherwood Sandstone Group: East Irish Sea Basin. *Geological Society, London, Special Publications*, **124**, 237–251, https://doi.org/10.1144/GSL.SP.1997.124.01.15

Tyrrell, S., Haughton, P.D., Souders, A.K., Daly, J.S. and Shannon, P.M. 2012. Large-scale, linked drainage systems in the NW European Triassic: insights from the Pb isotopic composition of detrital K-feldspar. *Journal of the Geological Society, London*, **169**, 279–295, https://doi.org/10.1144/0016-76492011-104

Underhill, J. and Stoneley, R. 1998. Introduction to the development, evolution and petroleum geology of the Wessex Basin. *Geological Society, London, Special Publications*, **133**, 1–18, https://doi.org/10.1144/GSL.SP.1998.133.01.01

Walsh, P.T., Collins, P., Ijtaba, M., Newton, J.P., Scott, N.H. and Turner, P.R. 1980. Palaeocurrent directions and their bearing on the origin of the Brassington Formation (Miocene–Pliocene) of the southern Pennines, Derbyshire, England. *Mercian Geologist*, **8**, 47–61.

Walsh, P.T., Banks, V.J., Jones, P.F., Pound, M.J. and Riding, J.B. 2018. A reassessment of the Brassington Formation (Miocene) of Derbyshire, UK and a review of related hypogene karst suffosion processes. *Journal of the Geological Society, London*, **175**, 443–463, https://doi.org/10.1144/jgs2017-029

Warrington, G. 1970*a*. The "Keuper" Series of the British Trias in the northern Irish Sea and neighbouring areas. *Nature*, **226**, 254–256, https://doi.org/10.1038/226254a0

Warrington, G. 1970*b*. The stratigraphy and palaeontology of the 'Keuper' Series of the central Midlands of England. *Quarterly Journal of the Geological Society*, **126**, 183–223, https://doi.org/10.1144/gsjgs.126.1.0183

Warrington, G. and Ivimey-Cook, H.C. 1992. Triassic. *Memoirs of the Geological Society of London*, **13**, 97–106, https://doi.org/10.1144/GSL.MEM.1992.013.01.11

Warrington, G. and Pollard, J.E. 2021. On the records of the brachiopod 'Lingula' and associated fossils in Mid-Triassic deposits in England. *Proceedings of the Yorkshire Geological Society*, **63**, https://doi.org/10.1144/pygs2020-015

Wills, L.J. 1956. *Concealed Coalfields: A Palaeographical Study of the Stratigraphy and Tectonics of Mid-England in Relation to Coal Reserves*. Blackie, London.

Wills, L.J. 1970. The Triassic succession in the central Midlands in its regional setting. *Quarterly Journal of the Geological Society*, **126**, 225–283, https://doi.org/10.1144/gsjgs.126.1.0225

Wills, L.J. 1976. *The Trias of Worcestershire and Warwickshire*. Report (Institute of Geological Sciences (Great Britain)), **76/2**. HMSO, London.

Wilson, A.A. 1990. The Mercia Mudstone Group (Trias) of the East Irish Sea Basin. *Proceedings of the Yorkshire Geological Society*, **48**, 1–22, https://doi.org/10.1144/pygs.48.1.1

Wilson, A.A. 1993. The Mercia Mudstone Group (Trias) of the Cheshire Basin. *Proceedings of the Yorkshire Geological Society*, **49**, 171–188, https://doi.org/10.1144/pygs.49.3.171

Wilson, A.A. and Evans, W.B. 1990. *Geology of the Country Around Blackpool*. Memoir of the British Geological Survey, Sheet 66 (England and Wales).

Wrobel-Daveau, J., Nicoll, G., Tetley, M.G., Gréselle, B., Perez-Diaz, L., Davies, A. and Eglington, B.M. 2022. Plate tectonic modelling and the energy transition. *Earth-Science Reviews*, **234**, https://doi.org/10.1016/j.earscirev.2022.104227

Yu9824 2021. Ternary Diagram, https://github.com/yu9824/ternary-diagram/ [last accessed 28 November 2024].